University of Stavanger

Faculty of Science and Technology

MASTER'S THESIS

Study program/specialization: Environmental Engineering, Water Science	Spring semester, 2010 Open access
Writer: Alexandra Renee Bausch	…… (Writer's signature)
Faculty supervisor: Roald Kommedal External supervisor(s): N/A	
Title of thesis: Biodegradation and chemical characterization of petroleum diesel hydrocarbons in seawater at low temperatures	
Credits (ECTS): 30 ECTS	
Key words: biodegradation diesel petroleum hydrocarbon marine seawater psychrophilic low temperature	Pages: 1-66 + Enclosure: 67-71 Stavanger, June 15, 2010 (Date/year)

Biodegradation and chemical characterization of petroleum diesel hydrocarbons in seawater at low temperatures

Alexandra Renee Bausch •

Faculty of Science and Technology, Department of Mathematics and Natural Science
Master of Science Degree Program, Environmental Engineering
University of Stavanger, Stavanger, Norway

• Telephone: +47 99886292; E-mail: alexandra.bausch@gmail.com

"Oh to follow the road that leads away from everything"
Pablo Neruda, "Casi fuera del cielo"

Acknowledgements

The research on diesel biodegradation was completed at the University of Stavanger in the Faculty of Science and Technology. Laboratory funding was provided by Total E&P Norge (UiS/Total cooperation agreement 2009). Sincere thanks to the US-Norway Fulbright Foundation for Educational Exchange. Thanks in advance to the Norway-American Association and the Norwegian Marshall Fund.

For the support in the laboratory, thanks to Roald Kommedal, Andrea Bagi, Gunn, and Stian. Thanks to Bente Dale and Torunn Buljo for administrative assistance. Thanks to the professors, teachers, colleagues, and peers who have expected more from me than I thought possible. Thanks to Dr. Grannas for the encouragement. Thanks to my dear friends, housemates, and family for the love and levity. To Andreas, thanks for it all.

Abstract

Petroleum hydrocarbons are a major source of marine contamination. Biodegradation, which is fundamental for the natural attenuation of these hydrocarbons in nature, involves mineralization or transformation of organic compounds by autochthonous microorganism communities. Various limiting factors characteristic of the petroleum, the external environment, and the microbial community determine the fate of oil (e.g., diesel) in the marine environment. Here, laboratory biodegradation experiments were conducted to investigate the aerobic biodegradation and chemical utilization of petroleum diesel hydrocarbons in seawater at four different temperatures: 15, 8, 4, and 0.5°C. Diesel, the sole carbon source, was immobilized on Fluortex adsorbents in closed-bottle microcosms. Biological oxygen demand was monitored via respirometric measurements over a period of 64 days. Designated test flasks were removed from incubation at various times for extraction, bacterial sampling, or total organic carbon analysis. Chemical degradation of the individual diesel hydrocarbons was monitored via liquid-liquid extraction in pentane, evaporation, and gas chromatography analysis. Based on chemical and bacterial analyses of diesel biodegradation, it was determined that incubation temperature affected petroleum diesel biodegradation. Rates of diesel biodegradation were enhanced at 15°C and retarded at 0.5°C. According to calculated half-life values for diesel hydrocarbon constituents, the rates of utilization were directly proportional to temperature and inversely proportional to hydrocarbon chain length. The method for chemical analysis caused significant evaporative losses of volatile hydrocarbon diesel fractions (64%). For both biodegradation and chemical utilization, the final extent of degradation was not affected by temperature. Future research is recommended to better understand biodegradation in natural systems.

Table of contents

List of figures

List of tables

Abbreviations

AODC: acridine orange direct count

BOD: biological oxygen demand

COD: chemical oxygen demand

DAPI: 4',6-diamidino-2-phenylindol

FID: flame ionization detection

GC: gas chromatography

HC: hydrocarbon

IRIS: International Research Institute of Stavanger

MPN: most-probable-number

MPS: multipurpose sampler

MS: mass spectrometry

NAPL: non-aqueous phase liquid

NPOC: non-purgeable organic carbon

THC: total hydrocarbons

TOC: total organic carbon

1 INTRODUCTION

Hydrocarbons (HCs) are organic compounds consisting of carbon and hydrogen, typically classified according to structure and bonding. In seawater, some hydrocarbons present are derived naturally from long-term geochemical transformations or biological processes (Widdel and Rabus, 2001). However, anthropogenic activities significantly contribute to HC accumulation in the oceans (National Research Council, 1985). In particular, petroleum hydrocarbons are a major source of marine pollution from crude oil and petroleum products (Deppe et al., 2005; Margesin and Schinner, 2001). Of the estimated 1.7 to 8.8 million metric tons of petroleum released into the ocean annually, over 80% originates from anthropogenic activities (National Research Council, 1985). Effluent release, industrial and municipal runoff, petroleum transport and spills, and shipping (Ibid) represent some significant input sources of petroleum products in marine environments.

Petroleum diesel is deposited into the ocean particularly during shipping activities and bilge or ballast cleaning practices (Geerdink et al., 1996; Michaud et al., 2004). Diesel is a fractional distillate of crude oil, composed of a complex mixture of HC fractions, principally saturated hydrocarbons (alkanes) and aromatic hydrocarbons (Margesin and Schinner, 2001; Michaud et al., 2004; Widdel and Rabus, 2001). Exact diesel HC composition is somewhat variable, depending on the distillation source (Leahy and Colwell, 1990). The hydrocarbon fractions present in diesel are also found in crude oil and other petroleum products.

Presently, petroleum pollution poses severe threats within marine environments. Extensive oil discharge may contaminate marine environments and shorelines (Figure 1-1), causing considerable localized destruction (Atlas, 1995). Moreover, some petroleum hydrocarbons, particularly the aromatic fractions, can cause serious health hazards for indigenous wildlife (Figure 1-2). Significant concentrations of petroleum HCs have been identified in marine organisms (Lee and Page, 1997; cited in Michaud et al., 2004; Walker et al., 2006). Numerous factors affect hydrocarbon toxicity in aquatic organisms, including the particular chemical present (i.e., chemical concentration, availability, and properties), the species affected, the environmental conditions, and the routes of uptake and excretion (Walker et al., 2006). Following HC exposure and uptake, primary biochemical responses may occur within marine organisms during enzymatic monooxygenase metabolism. Metabolic

activation of aromatic HCs can generate reactive intermediate metabolites that bind to cellular macromolecules, e.g., DNA (Ibid). DNA-adducts can cause formation of cancer cells, metastatic tumors, and lesions (Lee and Page, 1997; Walker et al., 2006). Secondary effects of hydrocarbon exposure on individual organisms include behavioral, developmental, and reproductive changes, which may lead to mortality (Ibid). Pollutant exposure may also culminate in population or community changes within the ecosystem.

A  B 

Figure 1-1. Onshore petroleum contamination from (A) Exxon Valdez oil spill in Alaska, 1989 and (B) fuel storage leakage in Lebanon, 2006 (www.britannica.com)

Figure 1-2. Wild mallard covered in oil following petroleum tanker spill in Korea, 2007 (www.boston.com)

The widespread toxicological effects of petroleum pollution may threaten numerous levels of biological organization. Thus, the fate of hydrocarbons within the marine environment is critically important. Following the discharge of petroleum in seawater, several natural weathering mechanisms disperse and degrade the component HC fractions (Atlas, 1981; Brakstad and Bonaunet, 2006; Lin et al., 2009). However, the removal of hydrocarbons via mechanical processes is often incomplete (Yang et al., 2000). The crucial, primary mechanism for physical attenuation via natural biological degradation is known as biodegradation (Atlas, 1995; Lindstrom and Braddock, 2002; Michaud et al., 2004). Biodegradation involves the metabolic transformation or complete mineralization of organic chemicals by autochthonous microorganisms (Aldrett et al., 1997; Margesin and Schinner, 2001). This complex process is affected by a variety of limiting factors

characteristic of the petroleum, the environment (e.g., temperature), and the microbial community (Leahy and Colwell, 1990). Bioremediation – a cleanup strategy – can be used to accelerate natural biodegradation rates by overcoming these limiting factors (cited in Margesin and Schinner, 2001; Rosenberg et al., 1992). However, in order for bioremediation efforts to be feasible and effective, the pathways of degradation and the underlying mechanisms for biodegradation kinetics must be understood.

Future environmental research regarding the fate and degradation of petroleum hydrocarbons is essential, especially in cold, high latitude regions due to increasing interest for oil exploration. Many recent studies have described petroleum hydrocarbon biodegradation in marine environments (Brakstad and Bonaunet, 2006; Delille et al., 2009; Deppe et al., 2005; Whyte et al., 1998). However, several of these investigations have focused on measuring biodegradation rates at temperatures above 20°C (cited in Deppe et al., 2005; Margesin and Schinner, 2001; Rosenberg et al., 1992) or reactions in soil or sediment matrices (Aislabie et al., 2006; Atlas, 1981; Lin et al., 2009; Mohn and Stewart, 2000; Powell et al., 2007). Few, however, have characterized petroleum diesel hydrocarbon biodegradation at low temperature in seawater (Michaud et al., 2004).

Hence, the aim of the present study is to investigate the aerobic biodegradation of diesel hydrocarbons in seawater at four different temperatures: 15°C, 8°C, 4°C, and 0.5°C. The research focuses on the chemical characterization and degradation of saturated and aromatic hydrocarbons, the principal constituents of petroleum diesel, as well as the overall degradation of total hydrocarbons (THC) during biodegradation. In the experiment, biological oxygen demand (BOD) by autochthonous microorganisms was monitored over a period of 64 days in closed-bottle systems. Throughout the experiment, chemical analyses of various diesel hydrocarbons were examined via liquid-liquid extraction in pentane and direct substrate gas chromatography with flame ionization detection (GC-FID). Mass spectrometry (MS) was used to analytically identify the diesel hydrocarbons in calibration. Total organic carbon (TOC) analysis was used to monitor degradation in positive controls.

The purpose of this biodegradation study is multifaceted. In the laboratory, quantitative biological and chemical analyses were performed to enhance understanding of diesel biodegradation in cold seawater. Broadly, the controlled biodegradation experiment herein was performed to model large-scale marine diesel spills (considering the limitations of

extrapolation to real world systems from microcosms) and to improve the present understanding of biodegradation within natural polar marine ecosystems. Moreover, temperature dependent studies were performed to illustrate biodegradation at various ocean temperatures. These trends may help forecast marine biodegradation rates with future ocean temperature changes associated with global warming (Brierley and Kingsford, 2009). Additionally, the experimental results may be used to simulate the biodegradation of crude oil and other petroleum products in low temperature seawater. These results may prove especially important with potential offshore petroleum development in high latitude regions. Furthermore, this biodegradation experiment may stimulate future research into biodegradation rate enhancement through bioremediation at low temperatures.

This report begins with an overview of biodegradation and remediation, specifically for petroleum hydrocarbons in low temperature seawater. Available methods for the analytical analyses of biodegradation are discussed briefly (Background). The experimental materials and methods utilized in the diesel biodegradation experiment are discussed in detail (Materials and methods). Experimental data and findings are then presented (Results) and evaluated (Discussion). The report concludes with a brief summary of the results and implications of diesel biodegradation (Conclusion). Supplemental theoretical and experimental information are included in Appendixes A and B, respectively.

2 BACKGROUND

Petroleum hydrocarbons represent a significant source of contamination in seawater and soil (Deppe et al., 2005; Margesin and Schinner, 2001). The biodegradation of these petroleum HCs in low temperature seawater depends on a synergy of complex, interrelated factors (Atlas, 1981; 1995). Field and laboratory studies have illustrated enhanced biodegradation rates in low temperature aqueous media, but many experiments cannot be extrapolated to natural systems (Delille et al., 2009; Michaud et al., 2004; Mohn and Stewart, 2000). Therefore, research is essential to better understand both the natural processes of microbial degradation in seawater at low temperature and the ultimate fate of petroleum hydrocarbons in natural ecosystems. With this knowledge, rates of degradation may be effectively enhanced through bioremediation.

This background provides an overview of the biodegradation of petroleum hydrocarbons in cold seawater. Following a short introduction to petroleum hydrocarbon biodegradation, various limiting factors (abiotic and biotic) are described in detail. Specifically, the fate of petroleum in the marine environment depends on properties characteristic of the petroleum, the ambient environment, and the microbial community. Next, several bioremediation strategies are introduced to enhance awareness of remediation practices. The chapter concludes with a brief description of some common methods for quantitative analyses of biodegradation.

2.1 Biodegradation

Biodegradation is the process by which autochthonous microorganisms mineralize or transform organic chemicals into simpler substances (Aldrett et al., 1997; Margesin and Schinner, 2001). Biodegradation is fundamental for the attenuation of petroleum hydrocarbons in nature (Atlas, 1995; Lindstrom and Braddock, 2002; Michaud et al., 2004). Pathways of degradation by microbial populations must be understood in order to predict the fate of hydrocarbons in the marine environment.

2.2 Chemical and physical factors affecting petroleum hydrocarbon biodegradation

The recalcitrance and fate of petroleum within an ecosystem is affected by a variety of abiotic factors. Rates of chemical utilization are contingent on the chemical and physical properties of both the proximate hydrocarbon fractions and the external environment.

2.2.1 Chemical composition

Crude oil and petroleum products (e.g., diesel) are composed of complex mixtures of hydrocarbons including alkanes, aromatic hydrocarbons, asphaltenes, and resins (Leahy and Colwell, 1990). The various HC fractions biologically degrade at different rates, according to chemical structure. Typically, saturated hydrocarbons biodegrade most rapidly, followed by branched alkanes and low molecular weight aromatics (Aldrett et al., 1997; Jobson et al., 1972; Leahy and Colwell, 1990). The slowest and most recalcitrant fractions include high molecular weight aromatics, resins, and asphaltenes (Ibid). This preferential chemical utilization depends on the hydrocarbon-degrading microorganisms

present (refer to 2.3). At the onset of petroleum biodegradation, microorganisms rapidly and preferentially degrade the low molecular weight fractions as sources of carbon and energy (Atlas, 1995; Jobson et al., 1972). As the degradation proceeds, mineralization rates decrease as high molecular weight and complex residual fractions accumulate (Ibid).

The principal components in petroleum are the saturated hydrocarbon fractions (Margesin and Schinner, 2001; Widdel and Rabus, 2001). Several recent studies show that short chain alkanes are metabolized faster than long chain hydrocarbons at low temperature (Deppe et al., 2005; Jobson et al., 1972; Lin et al., 2009; Lindstrom and Braddock, 2002; Whyte et al., 1998). According to Jobson et al., the low molecular weight, saturated hydrocarbons of crude oil degrade most rapidly and preferentially (1972). Saturated hydrocarbon utilization depends on the physical availability (i.e., bioavailability) of the chemicals for biodegradation (refer to 2.2.2). High molecular weight alkanes, for example, may form crystals at low temperatures, thereby decreasing bioavailability and increasing recalcitrance (Aislabie et al., 2006; Margesin and Schinner, 2001; Whyte et al., 1998).

2.2.2 Hydrocarbon concentration

Chemical concentrations can affect the biodegradation rates of numerous organic compounds. According to Monod microbial growth kinetics (Appendix A), the rate of mineralization is directly proportional to concentration (Leahy and Colwell, 1990). In petroleum hydrocarbon biodegradation, microbial growth presumably occurs on the dissolved HC fractions via Monod kinetics. Hence, the petroleum biodegradation rate is contingent on a myriad of factors including the HC solubility, equilibrium partitioning, and final soluble HC concentrations. Conversely, for some water insoluble compounds, biodegradation rates are concentration independent (Ibid).

2.2.3 Physical bioavailability

In petroleum biodegradation, hydrocarbons must be bioavailable – i.e., readily accessible for microbial attack. The physical state of oil affects bioavailability of the HC fractions. In high-energy aquatic environments, oil slicks may become horizontally dispersed and emulsified in the water column. Emulsions of oil in water serve to increase the surface area of exposed hydrocarbons at the interface of oil and water and therefore enhance bioavailability (Leahy

and Colwell, 1990). Conversely, large volumes of non-aqueous phase liquids (NAPLs) or weathered oil fractions decrease the available HC surface area for biodegradation (Ibid).

The relevant physical medium within an ecosystem (e.g., water or soil) also affects the bioavailability of petroleum hydrocarbons. Enhanced bioavailability is observed in aquatic environments, where oil slicks may become dispersed horizontally along the water surface (as mentioned above). In soil, petroleum becomes vertically entrapped in the physical matrix, thereby diminishing availability for biodegradation (Leahy and Colwell, 1990). Additionally, hydrocarbons may become absorbed or adsorbed to particulate matter in soil, further decreasing bioavailability (Aislabie et al., 2006; Leahy and Colwell, 1990). Other physical limitations in soil include low moisture content and drastic temperature fluctuations (Aislabie et al., 2006; Rosenberg et al., 1992).

2.2.4 Ambient temperature

Biodegradation rates generally decrease as ambient temperature decreases (Leahy and Colwell, 1990). This trend is consistent with the Arrhenius equation (Appendix A), which predicts that reaction rates should decrease exponentially as temperature decreases (Delille et al., 2009). The minimum threshold temperature for biodegradation in seawater is ≤0°C, since many petroleum hydrocarbons may form crystal structures at low temperatures (Aislabie et al., 2006; Margesin and Schinner, 2001; Whyte et al., 1998). Therefore, at very cold temperatures, some hydrocarbon fractions become recalcitrant.

In aquatic systems, temperature affects the physical weathering of oil, the bioavailability and partitioning of hydrophobic oil fractions, and consequently, the rates of hydrocarbon utilization (Brakstad and Bonaunet, 2006; Margesin and Schinner, 2001). At low temperature, the viscosity of the oil increases and the volatility of the hydrocarbon fractions decrease, thereby reducing bioavailability (cited in Leahy and Colwell, 1990; Margesin and Schinner, 2001; Michaud et al., 2004; Whyte et al., 1998). Temperature can also affect chemical solubility and consequent degradation efficiency (Ibid).

Moreover, temperature affects the metabolism and subsequent biodegradation rates and mineralization efficiency by indigenous microbial communities as well. Several studies indicate that biodegradation rates decrease with decreasing temperature, presumably

because of diminished enzymatic activities of autochthonous microorganisms (Deppe et al., 2005; Lin et al., 2009; Michaud et al., 2004; Whyte et al., 1998). According to Michaud et al., the biodegradation rates and efficiency for diesel in seawater are enhanced at high temperature (2004). Alternatively, Brakstad and Bonaunet (2006) claim that for naphthalene, only mineralization rates are significantly enhanced at high temperature (Figure 2-1, A). However, the final extent of naphthalene degradation is temperature independent (Figure 2-1, B). Similarly, Mohn and Stewart conclude that low temperatures significantly delay the HC biodegradation process in soil systems but do not ultimately affect the extent of transformation (2000). Conversely, Delille et al. maintain that temperature does not significantly affect the rates or the extent of crude oil mineralization in seawater (2009). Although the majority of experimental evidence indicates that biodegradation is likely temperature dependent, further investigations are necessary.

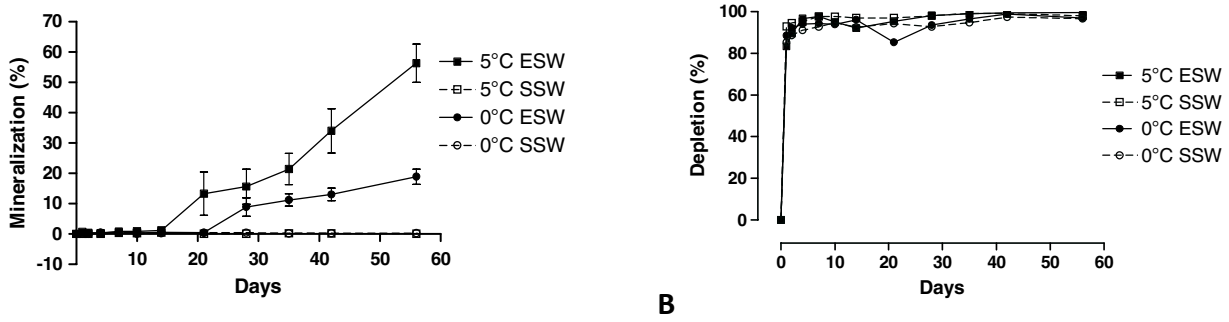

Figure 2-1. Naphthalene percent (A) mineralization and (B) depletion from oil-coated Fluortex adsorbents at 0°C and 5°C in nutrient-enriched (ESW) and sterile (SSW) seawater (Brakstad and Bonaunet, 2006)

2.2.5 Nutrient and oxygen availability

Hydrocarbon biodegradation is affected by nutrient and oxygen concentrations. In low temperature marine environments, biodegradation is primarily limited by the availability of inorganic nutrients (Atlas, 1995; Delille et al., 2009; Leahy and Colwell, 1990; Margesin and Schinner, 2001; Rosenberg et al., 1992). Specifically, nitrogen and phosphorous deficiencies are generally the rate-limiting factors for biodegradation (Ibid). Laboratory and field experiments by Rosenberg et al. indicate that the degradation of crude oil is enhanced in nutrient-enriched water (1992). Additionally, Mohn and Stewart maintain that dodecane mineralization rates in soil are significantly and necessarily enhanced by nitrogen and phosphorus addition (2000). Hence, nutrient supplements can be used to accelerate rates of biodegradation in aquatic systems (refer to 2.4.2).

Biodegradation is typically enhanced by increased oxygen availability since microbial utilization is preferentially aerobic (refer to 2.3.3). According to Jobson et al., the saturated hydrocarbons in crude oil degrade most rapidly with intense, continuous aeration (1972). In natural systems, rate limitation by oxygen availability is unlikely in high-energy or shallow marine environments, though possible in soil matrices (Leahy and Colwell, 1990).

2.2.6 Other abiotic environmental factors

In soil and seawater ecosystems, a variety of abiotic environmental factors (e.g., salinity, pH, and ambient pressure) can also affect biodegradation rates. Few studies have characterized the effects of ambient salinity on degradation rates (Leahy and Colwell, 1990). Generally, chemical utilization in saline environments depends on the adaptation and metabolism of autochthonous hydrocarbon degrading microorganisms (refer to 2.3). HC degradation can occur even in extreme saline environments. At high salt concentrations, halophilic and halotolerent species are known to mineralize a variety of organic compounds (Margesin and Schinner, 2001). According to Yang et al., diesel biodegradation occurs efficiently at salinities of 34, 36, 38, and even 40‰ (2000).

Typically, the optimal pH for biodegradation at low temperature is neutral or slightly basic. However, transformation can also occur in acidic environments via the metabolism of acidophilic species (Deppe et al., 2005; Leahy and Colwell, 1990; Margesin and Schinner, 2001). Extremely acidic environments can be deleterious to some HC biodegrading microorganisms (Kloos et al., 2006). Therefore, highly acidic or basic ambient pH may affect environmental persistence of petroleum hydrocarbons (Margesin and Schinner, 2001). If the pH in seawater is drastically altered from anthropogenic activities or global warming, biodegradation rates will be affected as well (cited in Margesin and Schinner, 2001).

The effects of pressure on rates of hydrocarbon degradation have only been studied in the depths of the ocean. In marine environments, some dense petroleum fractions can sink to the high-pressure benthic zone (Margesin and Schinner, 2001). Although biodegradation is possible in the deep-sea benthic environment (Leahy and Colwell, 1990), it proceeds very slowly due to low microbial activity at high pressure and low temperature (Margesin and Schinner, 2001). Additionally, recalcitrant petroleum fractions accumulate during chemical utilization by barophilic populations (Leahy and Colwell, 1990).

2.3 Biological factors affecting petroleum hydrocarbon biodegradation

Petroleum HC biodegradation also depends on a variety of biotic factors. The composition and biological nature of the autochthonous microbial populations affect the environmental recalcitrance of petroleum chemical fractions (Leahy and Colwell, 1990).

2.3.1 Hydrocarbon-degrading microorganisms

In aquatic environments, hydrocarbon biodegradation is performed by diverse populations of microorganisms (Atlas, 1995). Generally, bacteria are the primary HC-degraders in aquatic and soil environments, but fungi can also facilitate biodegradation (Atlas, 1995; Leahy and Colwell, 1990). Brakstad and Bonaunet identified predominantly bacterial degraders during HC biodegradation in Arctic seawater at low temperature (2006). Nonetheless, diverse populations of both hydrocarbon-degrading bacteria and fungi have been identified in marine and soil environments (Table 2-1).

In low temperature environments, petroleum hydrocarbon-degrading microorganisms generally adapt to ambient conditions (refer to 2.3.4). Cold-adapted HC-degraders include psychrophilic or psychrotrophic microorganisms, which have potential growth temperature ranges of 0 to 20°C and 0 to 35°C, respectively (Margesin and Schinner, 2001; Whyte et al., 1998). Typically, psychrotrophic populations contribute to biodegradation in Arctic and Antarctic regions (Aislabie et al., 2006; Margesin and Schinner, 2001; Michaud et al., 2004; Mohn and Stewart, 2000). Psychrotrophic species possess adaptive advantages for enhanced biodegradation at cold temperatures (Whyte et al., 1998).

Table 2-1. Examples of hydrocarbon-degrading microorganisms in marine/soil environments

Taxonomic group	Genus	References
Bacteria	*Achromobacter*	Atlas, 1981*; Leahy and Colwell, 1990*; Vieira et al., 2007
	Acinetobacter	Atlas, 1981*; Brakstad and Bonaunet, 2006; Leahy and Colwell, 1990*
	Agreia	Deppe et al., 2005
	Alcaligenes	Leahy and Colwell, 1990*
	Arthrobacter	Atlas, 1981*; Brakstad and Bonaunet, 2006; Leahy and Colwell, 1990*; Michaud et al., 2004
	Bacillus	Jobson et al., 1972; Leahy and Colwell, 1990*
	Flavobacterium	Atlas, 1981*; Jobson et al., 1972; Leahy and Colwell, 1990*; Nichols et al., 1999*
	Marinobacter	Deppe et al., 2005
	Nocardia	Atlas, 1981*; Leahy and Colwell, 1990*
	Pseudoalteromonas	Brakstad and Bonaunet, 2006; Deppe et al., 2005; Lin et al., 2009;
	Pseudomonas	Aislabie et al., 2006; Atlas, 1981*; 1995; Brakstad and Bonaunet, 2006; Deppe et al., 2005; Jobson et al., 1972; Leahy and Colwell, 1990*; Rosenberg et al., 1992; Vieira et al., 2007
	Psychrobacter	Deppe et al., 2005; Nichols et al., 1999*
	Rhodococcus	Aislabie et al., 2006; Michaud et al., 2004; Whyte et al., 1998
	Shewanella	Deppe et al., 2005; Nichols et al., 1999*
	Sphingomonas	Aislabie et al., 2006
	Vibrio	Atlas, 1981*; Leahy and Colwell, 1990*
Fungi	*Aureobasidium*	Leahy and Colwell, 1990*
	Aspergillus	Leahy and Colwell, 1990*
	Candida	Atlas, 1981*; Leahy and Colwell, 1990*
	Penicillium	Leahy and Colwell, 1990*
	Rhodotorula	Atlas, 1981*; Leahy and Colwell, 1990*
	Sporobolomyces	Atlas, 1981*; Leahy and Colwell, 1990*

*Cited in source

2.3.2 Growth

Microorganisms are ubiquitous in marine environments (Deppe et al., 2005; cited in Michaud et al., 2004). Indigenous HC-degrading species are present in variable amounts, but quantities are generally adequate for biodegradation (Delille et al., 2009; Leahy and Colwell, 1990). Immediately following petroleum contamination, the number of local hydrocarbon-degrading microorganisms increases rapidly. During chemical utilization, autochthonous species grow on hydrocarbon fractions due to increased numbers of hydrocarbon-utilizing plasmid genes in their populations (cited in Aislabie et al., 2006; Atlas, 1995; Delille et al., 2009; Leahy and Colwell, 1990; Margesin and Schinner, 2001).

Despite enhancement conditions, there is no proven direct relationship between microbial population size and percent hydrocarbon degradation (Aldrett et al., 1997).

Hydrocarbon-degraders can stimulate growth rates using either adhesion (Figure 2-2) or extracellular emulsification mechanisms to increase bioavailability (Atlas, 1981; Rosenberg et al., 1992). Although the microorganisms generally remain in the aqueous phase with nutrient supplies, the processes of adhesion, emulsification, and growth occur at the interface of oil and water (Ibid). Studies by Brakstad and Bonaunet indicate that bacteria in seawater adhere to oil prior to degradation (2006). Similarly, Deppe et al. describe bacterial adhesion to oil surface biofilms (Figure 2-3) before biodegradation initiation (2005).

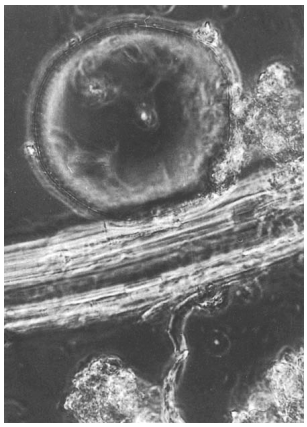

Figure 2-2. Phase micrograph showing adhesion of *Pseudomonas* to crude oil droplet after 3 days (Rosenberg et al., 1992)

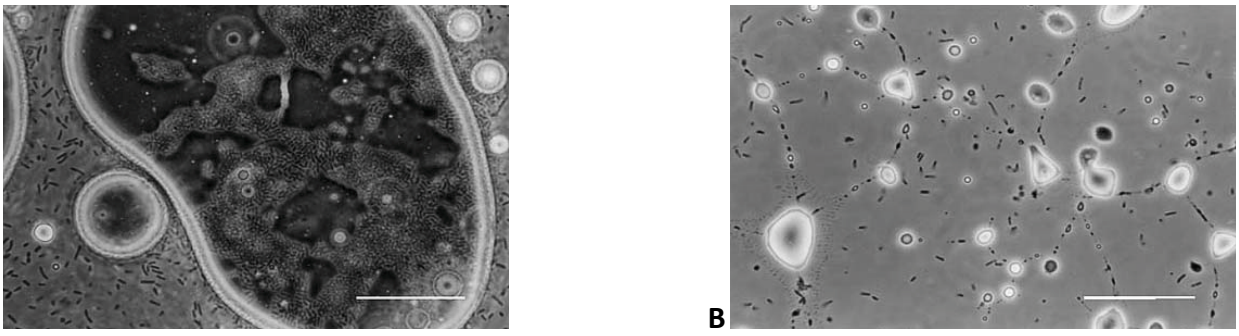

Figure 2-3. Micrograph showing bacterial adhesion and biofilm growth on oil droplets at 4°C after (A) 6 days and (B) 19 days (Deppe et al., 2005)
Scale: 10 μm

2.3.3 Metabolism

Individual microorganism strains can selectively metabolize a variety of hydrocarbons (Lin et al., 2009; Whyte et al., 1998). Hydrocarbon-degrading microorganisms may possess the enzymatic capacity to metabolize saturated hydrocarbons, aromatics, or both (Aislabie et al.,

2006; Leahy and Colwell, 1990). However, in order to metabolize complex assortments of hydrocarbons (e.g., diesel or crude oil), mixed microflora cultures are required (Deppe et al., 2005; Leahy and Colwell, 1990).

Enzymatic pathways for hydrocarbon degradation are encoded on plasmid or chromosomal genes (Atlas, 1995; Leahy and Colwell, 1990; Rosenberg et al., 1992). Several aerobic and anaerobic pathways for hydrocarbon oxidation have been identified in cold regions (Margesin and Schinner, 2001; Widdel and Rabus, 2001). In chemotrophic reactions (Figure 2-4), hydrocarbons are catabolized for energy and assimilated into protein biomass (Atlas, 1995; Widdel and Rabus, 2001). The initial steps in aerobic degradation involve oxygenase oxidation (Atlas, 1995; Leahy and Colwell, 1990; Rosenberg et al., 1992; Whyte et al., 1998). Biodegradation is preferentially aerobic but capable of proceeding slowly under anaerobic conditions (Atlas, 1981; Leahy and Colwell, 1990). Anaerobic oxidation involves novel mechanisms (Figure 2-4), which differ dramatically from aerobic processes (Widdel and Rabus, 2001).

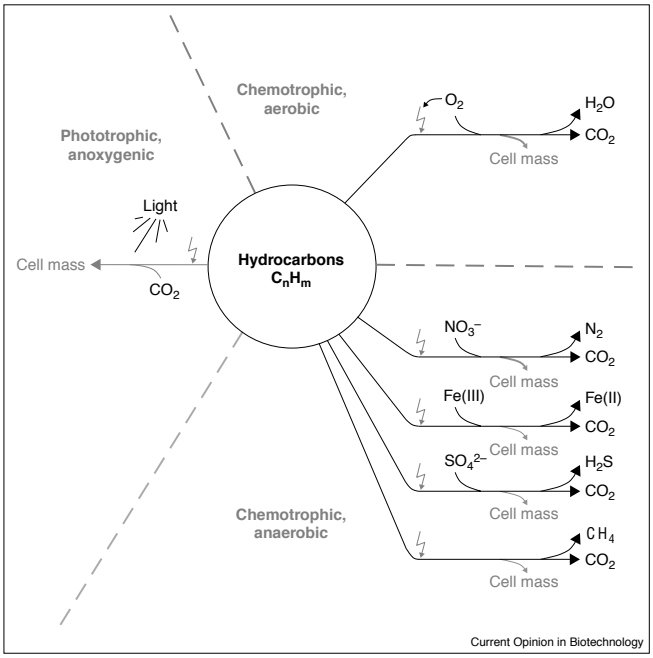

Figure 2-4. Potential pathways for hydrocarbon utilization by hydrocarbon-degrading microorganisms (Widdel and Rabus, 2001)

2.3.4 Adaptation

Microbial populations rapidly acclimate and adjust for environmental conditions and local contamination levels (Kloos et al., 2006; Margesin and Schinner, 2001). At low

environmental temperatures, cold-adapted enzymes exhibit adaptive flexibility for substrate degradation (Nichols et al., 1999). Microorganism communities exposed to significant hydrocarbon contamination have enhanced rates of HC oxidization (Atlas, 1981; Leahy and Colwell, 1990; Margesin and Schinner, 2001). Generally, the mechanisms for adaptation involve gene or enzyme modifications and selective enrichment of the microbial community (Leahy and Colwell, 1990). According to Atlas, the extent of previous exposures determines the ultimate success of biodegradation (1995). Many other studies indicate that the rate and extent of mineralization depend on previous exposure of the bacterial community to petroleum HCs (Leahy and Colwell, 1990; Margesin and Schinner, 2001; Yang et al., 2000).

2.4 Bioremediation

Bioremediation strategies are used to enhance natural hydrocarbon biodegradation. Optimal treatment conditions can be achieved through either induced or natural attenuation (Margesin and Schinner, 2001).

2.4.1 Bioaugmentation

Induced seeding – i.e., bioaugmentation – strategies involve the addition of allochthonous microorganisms to natural systems in order to enhance the rate or extent of biodegradation (Atlas, 1995; Leahy and Colwell, 1990). Unfortunately, the results of bioaugmentation are variable. Many studies do not illustrate enhanced degradation rates (Atlas, 1995), while others indicate slightly improved utilization rates after the addition of bioaugmentation agents (Aldrett et al., 1997; Whyte et al., 1998). However, in aquatic and soil systems, the locally adapted indigenous microorganisms tend to biodegrade substrates more effectively than foreign strains (Margesin and Schinner, 2001). Generally, the foreign strains are not able to adapt quickly enough to the given environmental conditions and are therefore easily outcompeted by the autochthonous members of the microbial community. Hence, further research and method development is essential for effective bioaugmentation.

2.4.2 Biostimulation

Natural environmental attenuation – i.e., biostimulation – involves the addition of chemicals to natural systems to enhance the conditions of biodegradation for native microbial populations (Aldrett et al., 1997). Several studies indicate that moderate concentrations of fertilizers stimulate biodegradation (Delille et al., 2009; Mohn and Stewart, 2000). Fertilizers supply nutrients, including nitrogen and phosphorus, to the oil-water interface (Figure 2-5), thereby creating optimal conditions for growth and ultimately enhancing rates of biodegradation (Atlas, 1995; Leahy and Colwell, 1990). However, at high concentrations, fertilizers can inhibit degradation (cited in Aislabie et al., 2006) and even cause serious ecological damage (e.g., eutrophication).

Artificial dispersants may also be used to enhance chemical degradation. Dispersants emulsify oil and increase the potential surface area for degradation (Leahy and Colwell, 1990; Margesin and Schinner, 2001). However, the results of biostimulation via dispersal addition are variable, depending on the dispersant used and the HC composition of the oil (Leahy and Colwell, 1990; Lindstrom and Braddock, 2002). Hence, additional research examining biostimulation methods in natural systems is imperative.

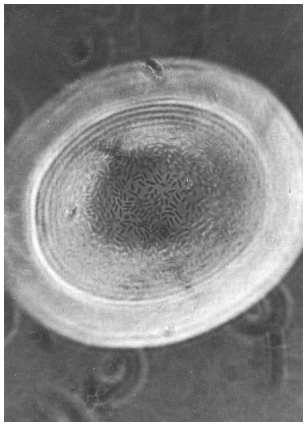

Figure 2-5. Phase micrograph showing adhesion of fertilizer to crude oil droplet in *Pseudomonas* culture (Rosenberg et al., 1992)

2.5 Quantitative methods for biodegradation analysis

Numerous analytical methods are available to monitor petroleum hydrocarbon biodegradation in seawater. Biological oxygen demand measurements can be used to indicate the oxygen demand by autochthonous microorganisms during HC degradation while chemical analyses during biodegradation can be used to examine the actual HC losses

over time. In addition, bacterial enumeration can be used to illustrate microbial growth enhancement conditions during chemical utilization.

2.5.1 BOD analysis

Biological oxygen demand is an index for the oxygen requirements of microorganism populations during the biodegradation of organic chemicals (e.g., petroleum). BOD is somewhat similar to chemical oxygen demand (COD), the oxygen required for complete chemical oxidation. BOD analysis typically involves indirect measurement of the molecular oxygen required for biological degradation of carbonaceous material over time. Since oxygen demand is proportional to carbon dioxide release by the microorganism community, some petroleum hydrocarbon BOD tests involve the quantification of carbon dioxide in the closed-system headspace (Brakstad and Bonaunet, 2006; Lindstrom and Braddock, 2002; Whyte et al., 1998). Other experiments involve pressure measurements in a sealed vessel since biological oxygen demand is inversely proportional to pressure (Appendix A; Kloos et al., 2006). Instrumental sensors (e.g., OxiTop control system heads) can be used to obtain respirometric pressure measurements in closed bottles during hydrocarbon utilization (*OxiTop System Control Operating Manual*, 2006). In BOD analysis, treatments, controls, and blanks are required (Aldrett et al., 1997; Whyte et al., 1998). Positive and negative controls are used to minimize the influence of false negatives and false positives, respectively. Blanks are used to indicate contamination during experimentation.

2.5.2 Chemical analysis

Gas chromatography (GC) and total organic carbon (TOC) analysis techniques are commonly used to evaluate chemical degradation of petroleum hydrocarbons. Extraction and sample preparation techniques can be used to prepare liquid samples for instrumental analysis via gas chromatography. Immiscible solvent extraction – or liquid-liquid extraction – is a technique used to separate compounds according to their relative solubility values in two immiscible liquid phases, typically water and an organic solvent (Mitra, 2003). Analytes (e.g., hydrocarbons) become distributed between the liquid compartments and may be recovered via multiple extractions of a single phase. Separatory funnels can be used to efficiently agitate and separate the two liquid layers. Concentrations of extracted analyte depend on the distribution coefficient (based on solubility), the volume ratio of the solvents,

and the number of extractions performed (Ibid). The standardized extraction method for hydrocarbon analysis involves liquid extraction from an aqueous phase to a single HC solvent phase (European Committee for Standardization, 2000). Examples of hydrocarbon extraction agents include hexane (Deppe et al., 2005; Vieira et al., 2007) and pentane (Jobson et al., 1972). Other extraction solvents for HC chemical analysis include dichloromethane (Aldrett et al., 1997; Delille et al., 2009) and diethyl ether (Whyte et al., 1998).

Following liquid extraction, samples may be concentrated to known volumes for quantitative gas chromatography analysis (Aldrett et al., 1997; Brakstad and Bonaunet, 2006; Delille et al., 2009). The standardized method for hydrocarbon analysis involves up-concentration with an evaporation apparatus (European Committee for Standardization, 2000). Samples can also be evaporated at ambient room temperature (Delille et al., 2009).

GC can be used to characterize the volatile organic fraction of petroleum following liquid-liquid extraction and concentration. In general, gas chromatography is used to separate, identify, and quantify the chemical constituents of volatile samples according to peak area responses (Dean, 1995). During injection, high temperatures are used to vaporize the sample. Chemical components are carried through the column by an inert mobile phase stream. In the column, the sample components interact variably with the stationary phase according to chemical affinity, ultimately causing chemical separation (Ibid). Various sensitive detectors can be used in GC, including thermal conductivity detectors and flame ionization detectors (FID). Some instruments are coupled to mass spectrometer (MS) detectors for identification and quantification of sample constituents by ion profile analysis. Data recorder devices generate outputs consisting of peak area responses based on retention times of the sample constituents.

GC-FID responses can be used to monitor the chemical degradation of both saturated and aromatic hydrocarbons (Brakstad and Bonaunet, 2006; Deppe et al., 2005; Geerdink et al., 1996; Jobson et al., 1972; Michaud et al., 2004; Vieira et al., 2007). Percent biodegradation efficiency can be determined from integrated peak area responses (Deppe et al., 2005; Michaud et al., 2004). GC-MS analysis can be used for the quantification and chemical classification of unidentified petroleum hydrocarbons (Delille et al., 2009; Lin et al., 2009; Lindstrom and Braddock, 2002; Powell et al., 2007; Whyte et al., 1998; Yang et al., 2000).

Total organic carbon analysis can be used to quantify the total amount of carbon present in a given sample. TOC quantification involves sample acidification, sparging, chemical oxidation, and detection. Responses from TOC analysis are used to monitor the total organic chemical degradation over time (Yang et al., 2000).

2.5.3 Bacterial analysis

Bacterial counts can be used to monitor microbial growth during biodegradation. Several standardized epifluorescence microscopy techniques are available for total bacterial enumeration (Sherr et al., 2001). Staining techniques commonly involve 4',6-diamidino-2-phenylindol (DAPI) or acridine orange direct count (AODC) epifluorescence microscopy (Brakstad and Bonaunet, 2006; Delille et al., 2009). The abundance of hydrocarbon-degrading microorganisms can be determined via the most-probable-number (MPN) technique, which involves serial dilutions to estimate bacterial density (Aldrett et al., 1997; Lindstrom and Braddock, 2002).

3 MATERIALS AND METHODS

Experimental methods were derived from those published in peer-reviewed literature sources (refer to 2.5). This chapter provides a detailed account of the techniques and necessary materials for the biodegradation and chemical characterization of petroleum diesel hydrocarbons.

All experimental glassware was scrubbed thoroughly, washed with Extran detergent (Merck, alkaline powder) in a laboratory dishwasher (Miele Mielabor Multitronic, G7783), and dried in an oven at 60°C (Termaks, B8054). Safety precautions were observed at all times.

3.1 BOD experiment

Aerobic diesel biodegradation was examined in low temperature seawater over a period of 64 days. At the onset of the experiment, the initial atmospheric pressure was 984 mbar. Throughout the experiment, oxygen demand was monitored via respirometric measurements in closed-bottle systems. Designated test flasks were removed from

incubation at various times for GC-FID, DAPI, or TOC analysis. For chemical analysis via GC-FID, test samples were extracted in pentane (C_5H_{12}) and up-concentrated to defined volumes. All mass measurements were obtained using an analytical balance (Sartorius, LE6202P).

3.1.1 Seawater source

Seawater was obtained from the International Research Institute of Stavanger (IRIS) at the Mekjarvik research facility in Randaberg, Norway. The North Atlantic compensation water was collected from a non-polluted fjord (59°1'N, 5°37'E) at a depth of 140 m, and was supplied through an intake pipe system of 70 m. At the time of collection, the water temperature was approximately 8°C, the salinity was 35.4‰, and the TOC was roughly 2 mg/L (from slowly biodegradable and inert fractions). Approximately 40 L of water was filtered to remove particulate matter, collected in autoclaved 10-L carboys (Nalgene, 2235), and stored at 5°C. With the exception of three time-zero solutions, the water was used within several hours of collection (refer to 3.1.3). No microbial inoculum was added prior to the biodegradation experiment. The density of seawater was assumed to be 1.035 g/mL. The microorganism community was assumed to be predominantly bacterial in composition. Additionally, it was assumed that a constant density of (hydrocarbon-degrading, psychrophilic) bacteria was present in all flasks during the biodegradation experiment.

3.1.2 Carbon source

In the biodegradation test flasks, the sole carbon source for microbial utilization was petroleum diesel. Standard, commercial grade diesel was obtained from a gas station in Stavanger, Norway. The average chemical formula was assumed to be $C_{16}H_{34}$ (assuming 70% saturated hydrocarbon composition), with a density of 0.75 g/mL, COD of 3.4 g O_2/g diesel, and BOD of 1.5 g O_2/g diesel. In the positive control flasks, sodium benzoate was used as the carbon source ($C_7H_5O_2Na$, Merck). The COD of sodium benzoate was calculated to be 1.61 g O_2/g sodium benzoate.

3.1.3 Experimental setup

All glassware used in BOD analysis was washed and autoclaved (Tuttnauer, 5075). Fluortex adsorbent screen fabrics (50 μm) were cut into circles of 18 mm diameter using a chisel hole punch, with an estimated deviation of 10%. Filters were washed thoroughly in pentane (VWR, OmniSolv, technical grade) and dried at room temperature. Solutions were prepared in 510 mL amber bottles with stir bars (3.8 cm length, 0.8 cm diameter) and rubber sleeve inserts (OxiTop). At each of four incubation temperatures (15, 8, 4, and 0.5°C), 14 bottles were analyzed: 10 parallel test flasks, 2 positive controls, 1 negative control, and 1 blank.

Solutions were prepared in 300 mL seawater. Water was measured by mass difference on the weighing balance, accounting for seawater density (1.035 g/mL) and nutrient addition volume (3 mL). Approximately 307 g of water was added to each bottle. All solutions contained 0.75 mL of nutrient solutions A, B, C, and D (provided by instructor), 10 μL of amino acids (Sigma Aldrich, Amino Acids Mix, RPMI 1640), and 10 μL of vitamins (Sigma Aldrich, MEM Vitamin Solution). Nutrient solutions were transferred via micropipette (Biohit, m5000, 500-5000 μL). To absorb carbon dioxide during biodegradation, 1 sodium hydroxide tablet (NaOH, Merck, solid pellet) was added in the rubber sleeve insert above the solution liquid level using metal tweezers.

In the diesel test flasks and negative controls, 24 μL of diesel, directly applied to Fluortex fabrics via glass syringe (Agilent, 50 μL, manual syringe), was added carefully to the liquid solutions. The initial diesel concentration was 200 mg/L COD (60 mg/L diesel). In the negative control flasks, 1 g of sodium azide (NaN_3, Merck, extra pure) was also added to eliminate hydrocarbon-degrading microorganisms in the sample. In the positive controls, 1 mL of sodium benzoate solution in pentane (105.3 mg/L) was added. Blank Fluortex fabrics were also added. The initial benzoate concentration was 199 mg/L COD (124 mg/L sodium benzoate). In the blank solutions, only clean Fluortex fabrics were added.

Three additional time-zero BOD flasks were prepared in order to analyze the initial extract HC concentrations prior to biodegradation. The initial condition solutions were prepared in the same manner as the negative controls. The seawater used in sample preparation was stored at 5°C for 4 months. Sodium azide was added to minimize the effects of HC-degrading microorganisms at time zero.

Systems were fitted with pressure sensors (OxiTop-C measuring heads, WTW) and sealed tightly to measure the pressure changes associated with oxygen consumption (Figure 3-1). All bottles were placed in incubators (Termaks, B8420) on inductive stirring systems (OxiTop, IS6). The experimental flasks were incubated at 15, 8, 4, and 0.5°C for 64 days with continuous stirring. The three initial condition flasks were incubated at 15°C for only 24 hours. The 15°C incubator was inadvertently unplugged on days 5-7. The OxiTop controller discontinued data collection on days 28-34. Throughout the BOD analysis, designated test bottles were removed from incubation for chemical or bacterial analysis. Data output was monitored and evaluated using the Achat OC software program.

Figure 3-1. OxiTop system setup for respirometric BOD analysis (www.labunlimited.com)

3.2 Sample preparation for GC analysis

In order to analyze hydrocarbon degradation via gas chromatography, experimental seawater samples were extracted and evaporated to specified volumes. Liquid-solvent extractions (3x) in pentane were performed using a Florisil/sodium sulfate column. Up-concentrations were performed using an elaborate evaporation apparatus setup.

3.2.1 Liquid-solvent extraction

All glassware and tools used in extraction were washed, dried, and rinsed with pentane. The pentane used in extraction was supplied by VWR (OmniSolv, technical grade). The boiling point of pentane was 36°C and the density was 0.63 g/mL. Hydrocarbon extraction was performed according to the general guidelines of the European Committee for Standardization (2000). During BOD analysis, random sample bottles were sacrificed for hydrocarbon analysis via extraction in pentane. Individual flasks were removed for extraction on days 3, 4, 5, 7, 12, 38 (15°C); days 5, 7, 17, 38, 45, 56 (8°C); days 17, 35, 42, 49, 56 (4°C); and days 21, 35, 42, 49, 56 (0.5°C).

Three extractions were performed for each flask. Following removal of the amber test vial from incubation, 20 mL of pentane was added and the system was stirred vigorously for 30 minutes on a magnetic stir plate (MSH basic, IKA). The entire liquid contents, along with the Fluortex adsorbent fabrics, were then poured into a 500 mL separatory funnel. Extraction was performed by shaking (12 repetitions), occasionally releasing the pressure by turning the stopcock. The solution in the separatory funnel rested for 5 minutes to allow complete separation of the water and pentane phases. If an emulsion was formed during the first extraction, 25 g of magnesium sulfate ($MgSO_4$, VWR, technical grade) was added. The denser aqueous phase (1.035 g/mL) was then drained into a clean 500 mL Erlenmeyer flask. The less dense pentane phase (0.63 g/mL) was drained into a 50 mL separatory funnel. The aqueous phase was returned to the 500 mL separatory funnel.

In the second and third extractions, 20 mL of pentane was added to the original amber BOD flask (via 100 mL glass graduated cylinder) and swirled gently to wash the bottle interior and stir bar surfaces. The pentane was then transferred to the Erlenmeyer and swirled carefully to wash the flask. Finally, the solvent was added to the 500 mL separatory funnel and extraction was performed via shaking, as described for the first extraction. The aqueous phase was recycled and the pentane phase was collected in the 50 mL separatory flask.

Residual aqueous liquid in the 50 mL separatory flask (if present) was drained and discarded. A glass column with a fritted funnel was prepared with approximately 2 g Florisil (Merck, 0.150-0.250 mm, column chromatography grade) and 2 g of sodium sulfate (Na_2SO_4, Merck, anhydrous, coarse granule), and was carefully rinsed with 10 mL of pentane without agitating the surface. The extracted pentane fraction was added slowly to the glass column and the filtered extract was drained into a glass bottle with a Teflon coated cap. The column was flushed with 10 mL of pentane. Final extracts (approximately 70 mL) were sealed tightly and stored in the refrigerator (Zanuzzi) at 4°C. Due to various technical difficulties in the laboratory, the extracts were stored for extensive periods in the fridge (2-3 weeks) prior to volume concentration.

3.2.2 Up-concentration

All glassware used in evaporation was rinsed with pentane prior to use. Pentane was obtained from VWR (OmniSolv, technical grade) or Merck (Unisolv, trace analysis grade). The up-concentration procedure was optimized using variable system parameters (e.g., temperature, pressure) with blank pentane samples.

The evaporation apparatus was outfitted with a circulating bath, a vacuum, a secondary condenser, and Büchi Syncore thermo-regulated evaporation vessels (Figure 3-2). The circulating bath (VWR, 1180S) contained about 6 L of antifreeze (Biltema, Standard), 3.5 L of ethylene glycol ($C_2H_6O_2$, Merck, Emplura), and approximately 14 L of tap water. A bath controller (VWR) was used to set the temperature of the coolant to -5°C. The vacuum pump (VWR, V-700) was fitted with a Woulff bottle solvent reservoir at the rear of the instrument. A vacuum controller (VWR, V-855) was used to regulate system pressure with a manual gradient pressure program. System pressure was set to 650 mbar for 35 minutes, then 600 mbar for 45 minutes. The secondary condenser (Büchi, Type-S) was fitted with a 2000 mL round-bottom collection flask. The evaporation apparatus (Büchi Syncore System, E20) included a 6-position rack with 6 interchangeable glass tubes (Crystal R-6) for parallel evaporation to 0.3 mL. To prevent evaporation to dryness, the tubes featured cooling zones at the level of the predefined residual volume. During up-concentration, the glass walls were rinsed with pentane using the flush-back function. Tubes were positioned above water baths (Milli-Q deionized water) heated to 50°C. Samples were aerated and rotated at a speed of 100 rpm. Evaporation progress in the samples was inspected after 35 minutes. Due to technical safety issues in the laboratory, a breathing protection mask with a gas filter was used during up-concentration (Dräger, 900).

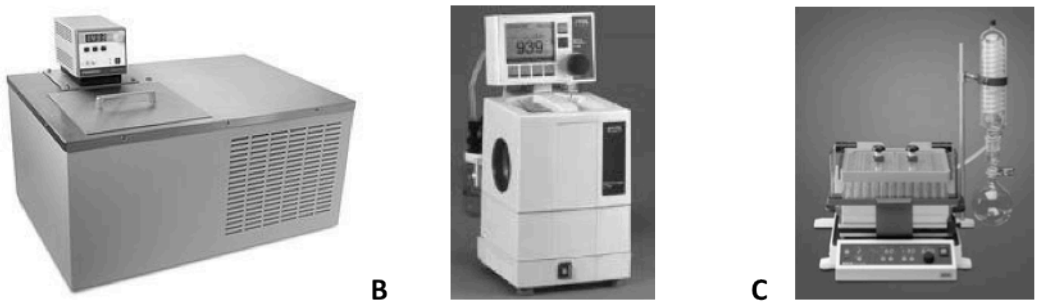

Figure 3-2. Evaporation setup including the (A) circulating bath (www.vwrsp.com), (B) vacuum pump (www.vwrcanlab.com), and (C) parallel evaporator with secondary condenser (www.mybuchi.com)

For sample up-concentration, extracted solutions were removed from refrigeration. To monitor recovery, a concentration standard solution of 2-fluorobiphenyl ($C_{12}H_9F$, Merck-Schuchardt, synthesis grade) was added to each extract. The solution (240 mg/L) was prepared with 0.024 g of 2-fluorobiphenyl in 100 mL of pentane. All extracts were supplemented with 10 µL of this concentration standard solution via glass syringe (Agilent, 50 µL, manual syringe), with the exception of flasks 23, 36, and 50. Solutions were swirled gently and added to individual glass evaporation tubes in the crystal rack. Extract bottles were rinsed with 10 mL of pentane (via graduated glass cylinder) for optimal recovery. The Büchi Syncore system was sealed and the vacuum program (described above) was turned on. Samples were inspected for evaporation progress after 35 minutes but the average time for complete evaporation was 45 minutes. Once evaporated to the predefined volume of 0.3 mL, the sample was transferred to a 2 mL glass volumetric flask via disposable glass pipette. The crystal tube was rinsed twice with pentane and the solution was diluted to 2 mL. The final concentration of 2-fluorobiphenyl standard in the 2 mL volumetric flask was 1.2 mg/L. Solutions were added to glass, amber autosampler vials (2 mL) fitted with polypropylene screw caps and Teflon septa for GC-FID analysis.

3.3 GC analysis

Following the liquid-solvent extraction and up-concentration of designated BOD flasks, samples were examined via GC-FID or GC-MS. In order to quantify the petroleum diesel hydrocarbons in the extracts, all relevant chemicals were identified and calibrated.

The GC (Agilent) was equipped with an inert mass selective detector and a Gerstel multipurpose sampler (MPS). The software integrator program (ChemStation, 6890) was

used to monitor the integrated peak area responses and resultant chemical concentrations throughout the BOD experiment. All samples were analyzed in amber glass autosampler vials (2 mL) fitted with Teflon septa and polypropylene caps. Pentane blanks were analyzed at the start of every sequence, prior to any GC sample injections. Chemical analyses were performed according to instrument operating instructions (*MultiPurposeSampler Operation Manual*, 2000).

3.3.1 Method

Method development and optimization were performed prior to GC-FID calibration. Several variations in instrumental parameters (e.g., oven temperature, ramp, column flow) were tested to establish the most suitable GC-FID method. The optimized method had a sample run-time of 25.50 min, with adequate petroleum HC peak resolution.

GC-FID method parameters were configured for the injector, inlets, columns, oven, and detector. The injector used a universal syringe adapter (Gerstel), equipped with a glass syringe (Gerstel Australia, 10 µL). Immediately prior to sample injection, the syringe performed three fill strokes of test sample at a volume of 5.0 µL. Samples from the liquid autosampler rack (Tray 2, VT98) were injected in the rear sample inlet via automatic injection (Gerstel MPS). The sample injection volume was 2.0 µL, with a fill/eject speed of 50.00 µL/s and a viscosity delay of 2.0 s. Syringe air volume was set to 0.0 µL. Injection penetration depth was 30.00 mm and vial penetration was 29.00 mm. Following injection, the syringe was rinsed twice with pentane solvent (Sigma-Aldrich, purum grade or Merck, Unisolv, trace analysis grade) at a fill/eject speed of 50.00 µL/s.

The inlets used splitless injection with constant helium gas flow for trace level analyte quantification. The rear inlet had a heater temperature of 320°C, pressure of 9.40 psi, and total flow of 20.0 mL/min. The purge flow to the split vent was 100 mL/min at 3.00 min and the gas saver flow was 15.0 mL/min at 3.50 min. The front inlet (HP PTV) heater temperature was set to 200°C and held for 0.30 min, with a cryo timeout at 30.00 min. The system pressure was 2.08 psi, with a total flow of 18.3 mL/min. The purge flow to split vent was 2.0 mL/min at 2.00 min and the gas saver flow was 15.0 mL/min at 1.00 min.

The columns were composed of 5% phenyl methyl siloxane. Capillary column 1 (Agilent HP-5MS, 19091S) connected the front inlet and the MS interface. Column features included a maximum temperature of 325°C, nominal length of 29.7 m, nominal diameter of 250.00 um, and nominal film thickness of 0.25 μm. The front inlet and MSD detector were used in constant pressure mode with vacuum outlet pressure. The helium flow pressure was 2.08 psi, the flow volume was 0.6 mL/min, and the average velocity was 28 cm/s. Capillary column 2 (Agilent HP-5, 19091J) connected the back inlet and the FID. This column had a maximum temperature of 325°C, nominal length of 30.0 m, diameter of 320.00 um, and film thickness of 0.25 um. The back inlet and front detector were used in constant flow mode, with ambient outlet pressure. The helium flow pressure was 9.14 psi, the flow volume was 2.0 mL/min, and the average velocity was 33 cm/s.

The oven used stepwise temperature settings. The initial temperature of 40°C was held for 3.00 min, with an equilibration time of 0.20 min. Oven temperature was ramped at 20.00°C/min to 325°C and held for 7.00 min. The temperature was ramped again at 100.00°C/min to 350°C and held for 1.00 min. The post-run temperature was set to 40°C.

The front detector (FID) was set to a temperature of 325°C, with a hydrogen flow of 40.0 mL/min, airflow of 450.0 mL/min, and a makeup nitrogen gas flow of 45.0 mL/min. Both the flame and electrometer were turned on.

In order to identify several unknown chemical components of diesel, a supplementary GC-MS method was created. Most parameters were identical to the GC-FID method described above but several were altered slightly. The back inlet temperature and pressure were changed to 200°C and 1.68 psi, respectively. Front inlet pressure was lowered to 4.67 psi and temperature was increased to 320°C. Column 1 had a helium flow pressure of 4.67 psi, flow volume of 0.8 mL/min, and velocity of 33 cm/s. Column 2 had a helium pressure of 1.68 psi, flow of 0.3 mL/min, and velocity of 6 cm/s. The detector flame and electrometer were turned off. The MS instrument used total scan mode with a 3.00-minute solvent delay.

For peak integration of the component hydrocarbons and standards, the following parameters were used on ChemStation: The initial rejected peak response was 100 000, with an initial peak width of 0.02 units. Shoulder detection was turned off, with a threshold value of 5.0. The integrator was turned off at 0.001 min and turned on again at 5.00 min. To

resolve individual peaks, the baseline now function was set at 5.00 min and baseline valleys were turned on at 6.00 min.

3.3.2 Calibrations

Following method development and optimization, calibration standards were prepared for selected saturated hydrocarbons, aromatics, and relevant standards in glass volumetric flasks. Pentane (Sigma-Aldrich, purum grade) was used as the solvent in solution preparation. Standard solutions were prepared with known hydrocarbon concentrations, analyzed via GC instrumental analysis (for retention time, peak area, and ion profile), and ultimately used to characterize diesel. All solutions were stored in amber bottles in the refrigerator (4°C). Validation was performed only for diesel THC (as opposed to each individual HC component) to verify the overall accuracy of GC-FID calibration.

Various saturated hydrocarbons present in diesel (C_9-C_{40}) were calibrated at 0.1, 0.5, 2, 5, and 10 mg/L from dilution of a stock solution. The stock solution of saturated hydrocarbons (2000 mg/L) was prepared in a 50 mL volumetric flask in pentane. The solid hydrocarbons (0.100 g) were dissolved directly in the solution. The liquid alkanes (0.100 g ÷ hydrocarbon density) were added to this solution via micropipette (Thermo Scientific, Finnpipette, 100-1000 µL). Table 3-1 displays the relevant chemical features for the liquid and solid saturated hydrocarbons included in the calibration solutions. The stock solution was then sonicated for 20 minutes at 50°C to dissolve any solid hydrocarbons. All solution volumes were transferred using a glass syringe (SGE Australia, 250 µL, manual syringe). The 10, 5, and 2 mg/L solutions were prepared in 100 mL of pentane with stock solution additions of 500, 250, and 100 µL, respectively. The 0.5 and 0.1 mg/L solutions were prepared in 10 mL of pentane with 500 and 100 µL additions of the 10 mg/L calibration solution, respectively.

The saturated HC solutions were directly analyzed via GC-FID. Retention time ranges were specified in the GC method integration parameters, based on the order of HC elution (with shorter chain alkanes eluting first). Linear calibration curves of response versus concentration were generated for each of the 18 saturated hydrocarbons.

Table 3-1. Chemical properties of the saturated hydrocarbons used in calibration solutions

State of matter at 20°C	Chemical	Formula	Supplier	Density (g/mL)
Liquid	nonane	C_9H_{20}	Merck-Schuchardt	0.718
	decane	$C_{10}H_{22}$	Merck-Schuchardt	0.729
	undecane	$C_{11}H_{24}$	Aldrich	0.740
	dodecane	$C_{12}H_{26}$	Riedel-de Haën	0.750
	tridecane	$C_{13}H_{28}$	Aldrich	0.755
	tetradecane	$C_{14}H_{30}$	Fluka	0.762
	pentadecane	$C_{15}H_{32}$	Aldrich	0.769
	hexadecane	$C_{16}H_{34}$	Riedel-de Haën	0.770
Solid	heptadecane	$C_{17}H_{36}$	Aldrich	N/A
	octadecane	$C_{18}H_{38}$	Aldrich	N/A
	nonadecane	$C_{19}H_{40}$	Aldrich	N/A
	eicosane	$C_{20}H_{42}$	Fluka	N/A
	docosane	$C_{22}H_{46}$	Aldrich	N/A
	tetracosane	$C_{24}H_{50}$	Fluka	N/A
	octacosane	$C_{28}H_{58}$	Fluka	N/A
	dotriacontane	$C_{32}H_{66}$	Fluka	N/A
	hexatriacontane	$C_{36}H_{74}$	Fluka	N/A
	tetracontane	$C_{40}H_{82}$	Fluka	N/A

Several aromatic hydrocarbons (benzene derivatives) present in diesel were calibrated at 0.1, 0.5, 2, 5, and 10 mg/L from dilution of an aromatic HC stock solution. The stock solution (2000 mg/L) was prepared in a 100 mL volumetric flask in pentane. The solid 1,2,4,5-tetramethylbenzene (0.200 g) was dissolved directly into solution. All other liquid hydrocarbons (0.200 g ÷ hydrocarbon density) were transferred to solution via micropipette (Thermo Scientific, Finnpipette, 100-1000 µL). Due to high volatility of the liquid aromatic hydrocarbons, the volumetric flask and stock bottles were sealed immediately after volume transfer. Table 3-2 includes the relevant chemical features of the aromatic hydrocarbons in the prepared solutions. The stock solution did not require sonication prior to solution preparation. The aromatic HC calibration solutions were prepared using the same volume transfers as in the alkane solutions, described above.

Aromatic hydrocarbons were calibrated via GC analysis. GC-MS was first used to identify individual peak responses and classify the order of elution for the aromatic hydrocarbons. GC-FID analysis was used to quantify the peak area responses based on the retention times

specified in the GC method integration parameters. Individual linear calibration curves were generated for each of the 9 aromatic hydrocarbons.

Table 3-2. Chemical properties of the aromatic hydrocarbons used in calibration solutions

State of matter at 20°C	Chemical	Formula	Supplier	Density (g/mL)
Liquid	benzene	C_6H_6	Fluka	0.879
	butylbenzene	$C_6H_5(CH_2)_3CH_3$	Aldrich	0.860
	ethylbenzene	$C_6H_5C_2H_5$	Fluka	0.867
	pentylbenzene	$C_6H_5(CH_2)_4CH_3$	Aldrich	0.859
	propylbenzene	$C_6H_5CH_2CH_2CH_3$	Aldrich	0.862
	toluene	$C_6H_5CH_3$	Fluka	0.867
	1,2,4-trimethylbenzene	$C_6H_3(CH_3)_3$	Fluka	0.867
	p-xylene	$C_6H_4(CH_3)_2$	Aldrich	0.866
Solid	1,2,4,5-tetramethylbenzene	$C_6H_2(CH_3)_4$	Aldrich	N/A

Three chemical standards were calibrated via GC-FID analysis. The branched hydrocarbons pristane ($C_{19}H_{40}$) and phytane ($C_{20}H_{42}$) were analyzed for potential use as internal standards for biodegradation and extraction recovery standards, respectively. Pristane and phytane were chosen since they are reportedly unbiodegradable at experimentally relevant conditions (Whyte et al., 1998). The fluorinated aromatic hydrocarbon, 2-fluorobiphenyl ($C_{12}H_9F$), was analyzed for potential use as a concentration standard during the evaporation procedure.

The stock solution of pristane and phytane (1000 mg/L) was prepared in 50 mL of pentane. Phytane (Fluka) was quantitatively transferred from a 50 mg bottle with several pentane rinses. To the 50 mL volumetric flask, 65 µL of pristane (Aldrich, density 0.783 g/mL) was transferred using a glass syringe (SGE Australia, 250 µL, manual syringe). The diluted calibration solution (2 mg/L) was prepared with 20 µL of stock solution in 10 mL pentane. Retention times for pristane and phytane were specified in the integration parameters to ensure proper resolution during diesel analysis. Linear calibration curves were constructed for each hydrocarbon standard based on responses from the 2 mg/L solution.

The stock solution of 2-fluorobiphenyl (240 mg/L) was prepared using 0.024 g of 2-fluorobiphenyl in 100 mL of pentane (refer to 3.2.2). Two calibration solutions (12 and 1.2 mg/L) were prepared in volumetric flasks. The 12 mg/L solution was made with 500 µL of

stock solution in 10 mL of pentane. The 1.2 mg/L solution was prepared using 250 µL of the stock in 50 mL pentane. The linear calibration curve was generated for 2-fluorobiphenyl based on GC-FID peak area responses from only the 12 mg/L solution (due to cross contamination in the 1.2 mg/L solution).

3.3.3 Chemical analysis of diesel

The chemical analysis of diesel was performed following the extensive GC-FID calibration of saturated hydrocarbons, aromatic hydrocarbons, and experimental standards. Diesel solutions in pentane were calibrated, validated, and characterized.

Diesel total hydrocarbons were calibrated via GC-FID analysis at 5000, 2000, 500, and 300 mg/L. Diesel was obtained from a petrol station in Stavanger, Norway (refer to 3.1.2). Solutions were prepared in 50 mL volumetric flasks and volumes were transferred via glass syringe (SGE Australia 250 µL or Agilent 50 µL manual syringe). The 5000 and 2000 mg/L solutions were prepared using 335 and 135 µL of commercial diesel in 50 mL pentane, respectively. The 500 and 300 mg/L solutions were prepared with 35 and 20 µL of diesel in 50 mL pentane, respectively. Samples were analyzed via GC-FID according to the optimized instrumental method (refer to 3.3.1). However, several integration parameters were modified slightly for diesel THC analysis.

The following parameters were used on ChemStation to quantify diesel THC: The initial rejected peak response was 100 000, with an initial peak width of 0.02 units. Shoulder detection was turned off, with a threshold value of 5.0 units. The integrator was turned off at 0.001 min and turned on again at 4.60 min. In order to integrate the entire diesel peak, the baseline now and hold functions were set at 4.64 min and the baseline valleys were turned off. Peak area summation was initiated at 5.85 min and then discontinued at 20.0 min. The integrator was turned off at 21.0 min.

The diesel THC calibration curve was generated from the total integrated peak area responses. Validation was performed to ensure accuracy of the GC-FID calibration. The validation solution (3750 mg/L diesel) was prepared using 50 µL of diesel in 10 mL pentane. The solution was analyzed directly via GC-FID analysis to compare the calibrated concentration to the known value.

Diesel chemical composition was characterized based on the GC-FID calibration curves of the alkanes, aromatic hydrocarbons, and experimental standards (refer to 3.3.2). The concentration of each chemical component was determined in the 300 mg/L stock solution of diesel in pentane (15 mg diesel in 50 mL pentane), described above.

3.3.4 BOD experiment hydrocarbon analysis

Petroleum hydrocarbon concentrations in the extracted, concentrated experimental samples were quantified via GC-FID analysis. The analysis was used to monitor chemical utilization via bacterial populations in seawater over time. Extracts were analyzed according to the optimized GC method used in the calibrations (refer to 3.3.1).

3.4 TOC analysis

Positive control BOD flasks were examined via TOC analysis. Based on sodium benzoate BOD curve progress, aliquots were regularly removed from positive control flasks for TOC sample preparation. Bottles were sampled on days 3, 4, 5, 6, 7 (15°C); days 3, 4, 5, 6, 7, 10, 11, 12, 14 (8°C); days 3, 5, 6, 7, 10, 11, 12, 14, 17, 19 (4°C); and days 3, 6, 7, 10, 11, 14, 19, 21 (0.5°C). Using a glass syringe (SGE Australia, 5 mL, manual syringe), 3 mL of seawater was extracted from each positive control flask. A syringe filter (Chromacol LTD, 0.2 µm, PES for ion chromatography) of 30 mm diameter was used to filter the bacteria from the sample. To clean the filter, 1 mL of sample was pushed through the filter and discarded. The remaining 2 mL of sample were filtered into 50 mL glass, screw-cap bottles. Blank TOC solutions were prepared using 2 mL of deionized water (Milli-Q). All samples were acidified by adding 200 µL of 2 M hydrochloric acid (HCl, VWR) via micropipette (Thermo Scientific, Finnpipette, 100-1000 µL). Bottles were fitted with plastic caps and stored in the refrigerator at 4°C.

To prepare samples for instrumental TOC analysis, glass TOC vials (30 mL) were soaked in 0.2 M HCl solutions, prepared by adding 3 mL of 2 M HCl via micropipette to each TOC bottle (Biohit, m5000, 500-5000 µL) and diluting with deionized water (Milli-Q). Vials were acidified for 4 hours and dried overnight in an oven at 300°C. For qualitative transfer of the refrigerated samples into the cleaned TOC bottles, 8 mL of water (Milli-Q) was added to each refrigerated vial via micropipette (Biohit, m5000, 500-5000 µL). Vials were shaken gently and poured directly into the cleaned, labeled TOC bottles. Samples were further

acidified by adding 500 µL of 2 M HCl (Thermo Scientific, Finnpipette, 100-1000 µL). The TOC bottles were capped with foil to prevent evaporative losses.

Instrumental analysis was performed using an Analytic Jena TOC analyzer (TOC 3100), previously calibrated using potassium phthalate (VWR) solutions (0.1 to 5 mg/L). The instrument was operated in non-purgeable organic carbon (NPOC) mode at a temperature of 850°C. TOC bottles in the sequence were arranged in reverse chronological order of sampling date (low to high TOC concentration). Each sample was acidified with 200 µL of 2 M HCl and sparged for 3 minutes with carbon-free air (synthetic air). Organic carbon in the sample (NPOC) was oxidized to carbon dioxide, which was measured and quantified three times per sample. Average and standard deviation values of TOC concentrations were reported for each solution.

3.5 DAPI analysis

Throughout BOD analysis, sample aliquots were removed from BOD bottles for future enumeration of microbial cells via DAPI staining and microscopy. Bottles were sampled on days 3, 4, 5, 6, 7, 12, 38 (15°C); days 3, 4, 5, 6, 7, 10, 11, 12, 14, 17, 38, 45, 56 (8°C); days 3, 5, 6, 7, 10, 11, 12, 14, 17, 19, 35, 42, 49, 56 (4°C); and days 3, 6, 7, 10, 11, 19, 21, 35, 42, 49, 56 (0.5°C). At each sampling time, three BOD flasks were analyzed per temperature. Two test bottles, designated for DAPI sampling only, were analyzed. Various positive control and test flasks were also analyzed when bottles were removed for TOC sample preparation and extraction, respectively. Sample aliquots of 2 mL were transferred to clean DAPI sample bottles via micropipette (Thermo Scientific, Finnpipette, 100-1000 µL) or glass syringe (SGE Australia, 5 mL, manual syringe). For bacterial fixation, 8 drops of 37% borate buffered formalin (VWR, solution prepared by advisor) was added via syringe (Hamilton Co., 1000 µL, gastight syringe) with a syringe filter attachment (Chromacol LTD, 0.2 µm, PES for ion chromatography). DAPI bottles were capped tightly and placed in a freezer at -18°C (Electrolux, Low Frost) for storage. DAPI staining, epifluorescence microscopy, and enumeration were not performed due to technical difficulties and time constraints. Solutions were prepared, however, for epifluorescence analysis in the near future.

4 RESULTS

The biodegradation and chemical characterization of petroleum diesel hydrocarbons were evaluated at low temperatures via BOD, GC, and TOC analyses. This chapter provides an account of all relevant experimental data and findings.

4.1 BOD analysis

Aerobic biodegradation was continuously monitored at various low temperatures via BOD analysis. Respirometric pressure measurements in closed bottles were used to quantify the oxygen requirements for biological degradation. Experimental test flasks were used to measure oxygen consumption by microbial consortia during biodegradation of diesel petroleum hydrocarbons. Positive controls were used to measure the BOD of sodium benzoate at various temperatures in order to verify the biodegradation protocol. Negative controls were used to identify abiotic or systematic fluctuations. Blank flasks were used to indicate potential contamination during the experiment.

Original BOD data from the control and test flasks were justifiably manipulated. All data values were compensated for abrupt fluctuations in BOD, which resulted from pressure changes in open bottles. When flasks were opened, BOD values were immediately adjusted according to the ambient atmospheric pressure. A distinctive negative correlation exists between normalized (dimensionless) BOD and atmospheric pressure data (Figure B-1, Appendix B). Several experimental BOD bottles exhibited significant BOD drift due to inadequate bottle closure, particularly before day 3. Therefore, data values were compensated and projected together, based on the trends of BOD increase observed in the original data from closed bottles. BOD values were then corrected using the compensated negative control as a stable reference. In other words, the compensated BOD values from blank, positive, and test flasks were corrected by subtracting the compensated BOD values from the negative controls. Final BOD values were then calculated for positive control and test flasks by subtracting corrected blank values from corrected BOD values. Compensated, corrected data for the control and diesel test flasks were plotted graphically as parallels for every temperature.

4.1.1 Control and blank flasks

BOD values from blank, positive, and negative control flasks were compensated for abrupt variation and corrected (refer to 4.1). Abrupt pressure changes were specifically observed when the positive control flasks were sampled for TOC and DAPI analysis. Data from positive controls and blanks were corrected using the compensated negative values as a stable reference. The corrected BOD values of the blank solutions increased slightly over time at 15, 8, and 4°C, indicating possible contamination during the experiment. The corrected BOD values at 0.5°C were subject to greater fluctuations. Final BOD values were used to construct BOD curves for sodium benzoate at each experimental temperature. Blank BOD values were also included in the graphs.

Figure 4-1 illustrates the BOD curves for sodium benzoate at 15°C. During days 5-7, the incubator was accidentally unplugged. Therefore, BOD data was deleted and projected according to the trend of BOD increase. Since the blank flask was not properly closed before day 3, blank data was excluded during days 0-3. Blank BOD data was repositioned at 0 mg/L on day 3. At 15°C, the exponential phase for bacterial growth during sodium benzoate biodegradation occurred approximately between 2 and 5 days.

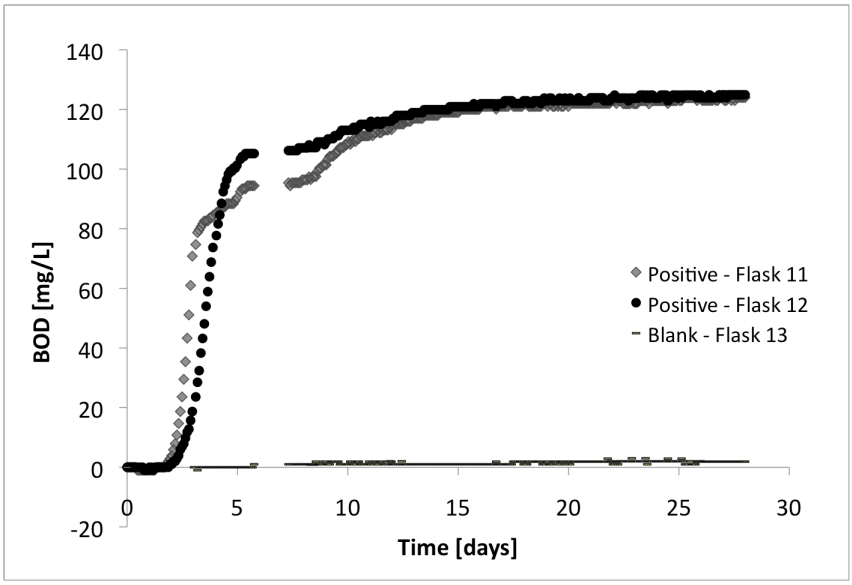

Figure 4-1. BOD curves of sodium benzoate at 15°C following data compensation and correction

The BOD curves for sodium benzoate at 8°C are shown in Figure 4-2. Both of the positive control flasks were accidentally open to ambient pressure fluctuations on days 0-3. Therefore, positive control BOD data was deleted prior to day 3, and the data was

repositioned at 0 mg/L on day 3. At 8°C, the exponential growth phase for sodium benzoate degradation occurred approximately between 7 and 12 days.

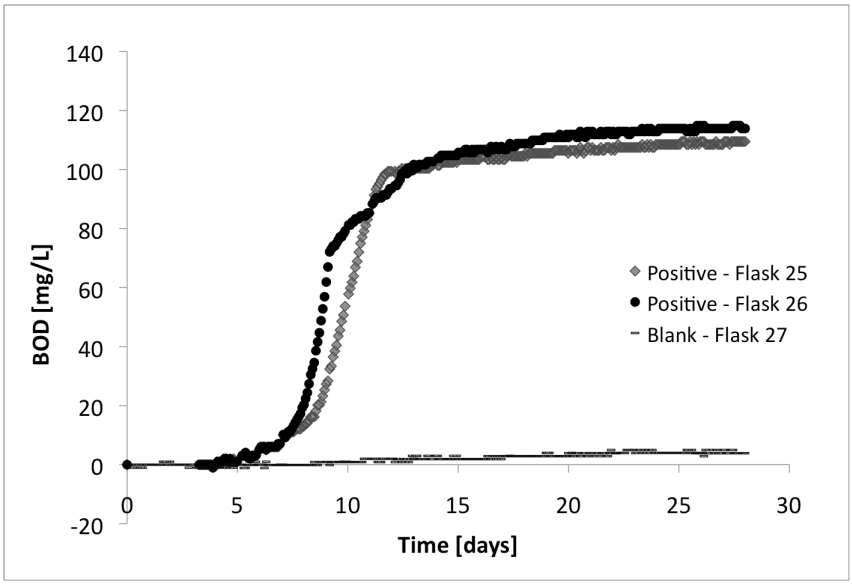

Figure 4-2. BOD curves of sodium benzoate at 8°C following data compensation and correction

The BOD curves for sodium benzoate at 4°C are depicted in Figure 4-3. One positive control flask (Flask 40) and the blank flask were unintentionally open at the beginning of the experiment. Data values were removed from days 0-3 and repositioned at 0 mg/L. At 4°C, the exponential growth phase during sodium benzoate utilization occurs between 7 and 16 days. The growth phase occurred slightly earlier in one positive control flask (Flask 39), compared to the other (Flask 40).

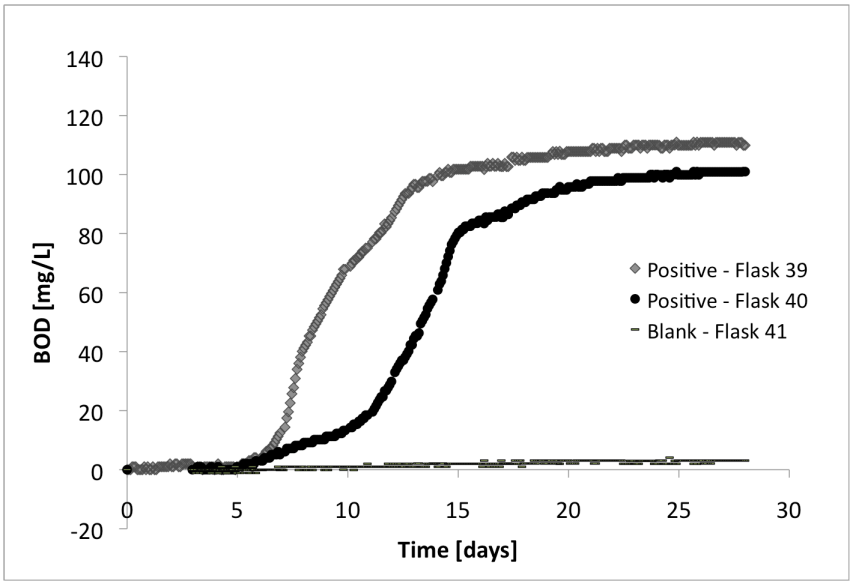

Figure 4-3. BOD curves of sodium benzoate at 4°C following data compensation and correction

The sodium benzoate BOD curves at 0.5°C are shown in Figure 4-4. One positive control flask (Flask 53) and the blank flask remained inadvertently open until day 3. Initial data was removed and repositioned at 0 mg/L on day 3. At 0.5°C, the exponential phase for sodium benzoate biodegradation occurs after 17 days. The growth phase occurred earlier in one particular positive control flask (Flask 53), compared to the other (Flask 54).

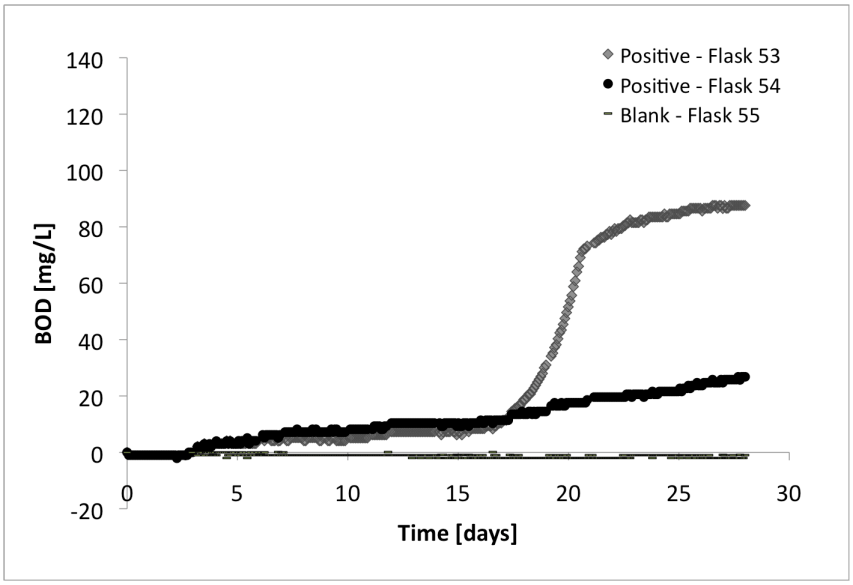

Figure 4-4. BOD curves of sodium benzoate at 0.5°C following data compensation and correction

4.1.2 Test flasks

BOD values from diesel test bottles were compensated and corrected (refer to 4.1). For the sake of simplicity, the reported BOD values were derived from unopened test flasks – those not used for extraction, TOC, or DAPI analysis. However, the BOD curves for all other flasks at a given temperature were similar up to the point of sacrifice. Experimental data were compensated for erratic fluctuations in pressure. If flasks were not properly sealed at a given temperature, data was modified according to the average BOD value from the closed bottles.

Since the experiment was inadvertently stopped for 7 days, BOD curves were mathematically (as opposed to biologically) projected. The equations of second order polynomial fits were used to extrapolate the data from days 28 to 35, assuming that the reaction proceeded normally. Using the compensated, corrected blank and negative values from BOD analysis (refer to 4.1.1), the final BOD values for diesel were calculated and depicted graphically. Growth parameters could not be determined by graphical analysis. The BOD curves could only be compared qualitatively (Figure B-2, Appendix B).

The BOD curves for diesel biodegradation at 15°C are depicted in Figure 4-5. Polynomial curves used in data extrapolation were generated from data on days 7-28.

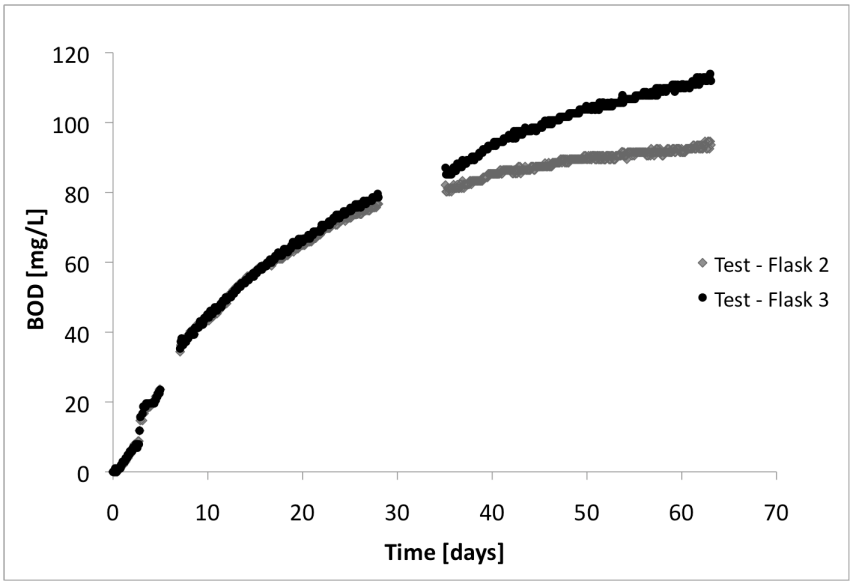

Figure 4-5. BOD curves of diesel at 15°C following data compensation, projection, and correction

Diesel BOD curves at 8°C are illustrated in Figure 4-6. One diesel test flask (Flask 19) remained unintentionally open before day 3. The BOD data was compensated using the average BOD from the sealed bottles on day 3. Polynomial curves from days 11-28 were used for extrapolation.

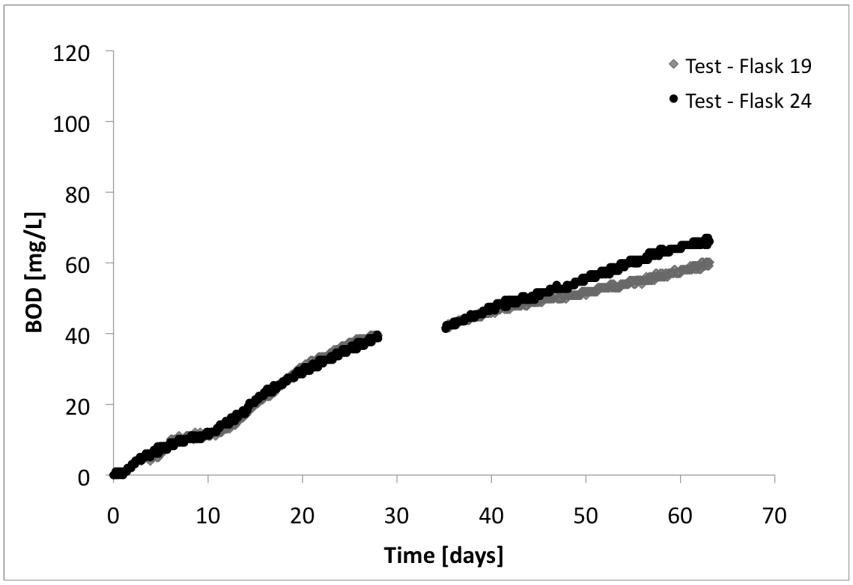

Figure 4-6. BOD curves of diesel at 8°C following data compensation, projection, and correction

The diesel BOD curves at 4°C are shown in Figure 4-7. One test flask (Flask 35) was not adequately sealed before 3 days. BOD data was corrected according to the average BOD

value from the sealed flasks at day 3. Curves for extrapolation were projected from the data on days 15-28.

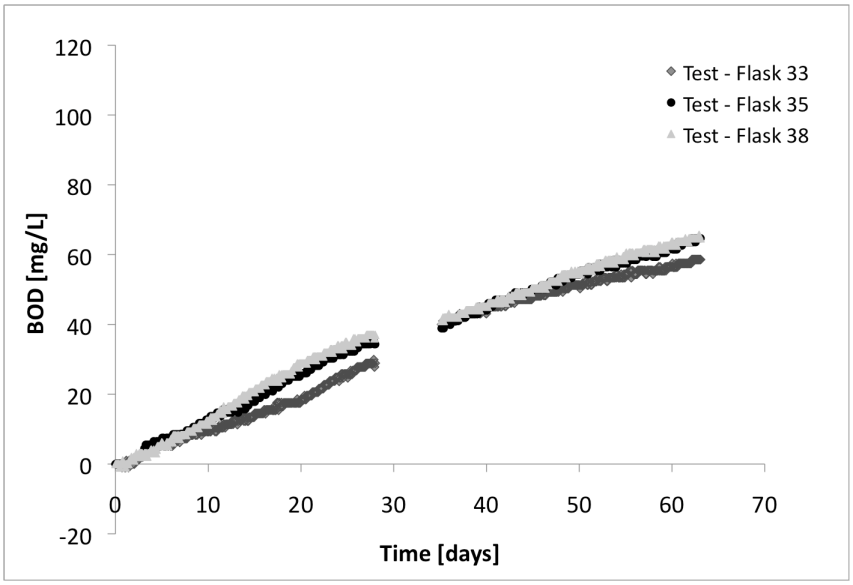

Figure 4-7. BOD curves of diesel at 4°C following data compensation, projection, and correction

The BOD curves for diesel biodegradation at 0.5°C are included in Figure 4-8. Two flasks (Flasks 51 and 52) were not properly sealed on days 0-3. Data was corrected using the average BOD value from the closed BOD flasks on day 3. Extrapolated polynomial curves were generated from BOD data on days 10-28.

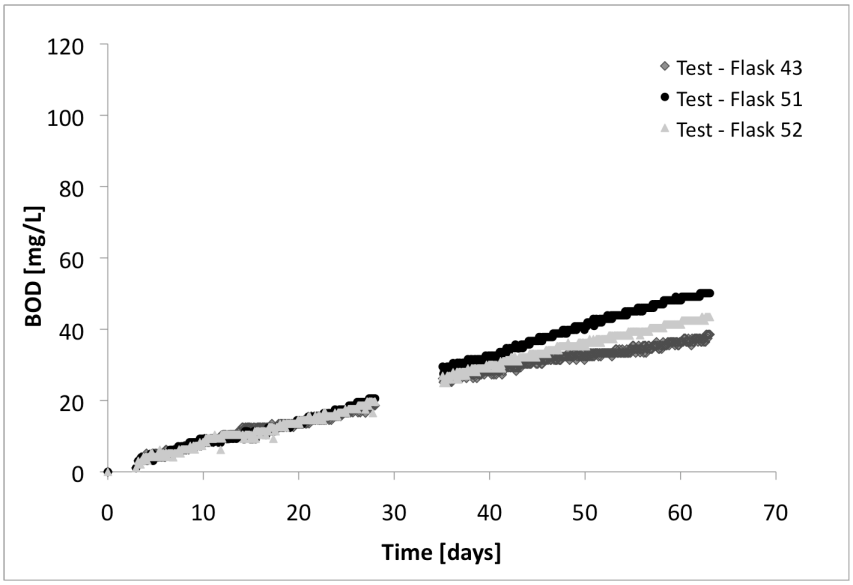

Figure 4-8. BOD curves of diesel at 0.5°C following data compensation, projection, and correction

4.2 GC analysis

Gas chromatography was used to monitor chemical utilization. Petroleum hydrocarbons, diesel THC, and chemical standards were calibrated and quantified via GC-FID and MS analysis.

4.2.1 Calibrations

GC-FID calibration results for saturated hydrocarbons, aromatics, and chemical standards were used to quantify the HC components of petroleum diesel. All samples were contaminated with autosampler septum phthalates, with peaks eluting consistently around 9.0 and 12.5 minutes. GC-MS analysis specifically identified diethylphthalate contamination at 12.55 minutes.

Saturated and aromatic hydrocarbons were calibrated at 0.1, 0.5, 2, 5, and 10 mg/L. Calibration curves for each hydrocarbon were linear, forced through the origin. Linear terms were similar for all chemical components due to the stability of the FID detector. Calibration results for the saturated hydrocarbons (e.g., retention times, linear terms, and r^2 values) are included in Table 4-1. Tetracontane was not identified on the calibration chromatograms at 0.1 and 10 mg/L. The average linear term for the alkanes was $2.4 \times 10^6 \pm 0.2 \times 10^6$.

Table 4-1. Summary of calibration results for saturated hydrocarbons

Chemical	Retention time (min)	Linear term x 10^{-6}	Coef. of det. (r^2)
nonane	5.679	2.62	0.9991
decane	6.739	2.10	0.9992
undecane	7.625	2.69	0.9992
dodecane	8.404	2.57	0.9991
tridecane	9.114	2.76	0.9991
tetradecane	9.774	2.65	0.9990
pentadecane	10.394	2.08	0.9994
hexadecane	10.979	2.40	0.9990
heptadecane	11.535	2.25	0.9990
octadecane	12.063	2.25	0.9990
nonadecane	12.568	2.24	0.9988
eicosane	13.050	2.41	0.9991
docosane	13.954	2.31	0.9988
tetracosane	14.788	2.22	0.9989
octacosane	16.425	2.31	0.9993
dotriacontane	17.603	2.34	0.9990
hexatriacontane	19.296	2.25	0.9998
tetracontane	22.229	2.33	0.9988

Aromatic hydrocarbons were identified via GC-MS and quantified using GC-FID. Calibration results for the aromatic hydrocarbons are included in Table 4-2. Benzene and toluene were not calibrated since they eluted in the pentane shoulder of the chromatograms and could not be identified or quantified. The average linear term for the viable aromatic hydrocarbons was calculated to be $2.6 \times 10^6 \pm 0.3 \times 10^6$.

Table 4-2. Summary of calibration results for aromatic hydrocarbons

Chemical	Retention time (min)	Linear term x 10^{-6}	Coef. of det. (r^2)
benzene	N/A	N/A	N/A
toluene	N/A	N/A	N/A
ethylbenzene	5.199	2.27	0.9990
p-xylene	5.324	3.09	0.9993
propylbenzene	6.304	2.35	0.9973
trimethylbenzene	6.699	2.49	0.9988
butylbenzene	7.292	2.69	0.9989
tetramethylbenzene	7.800	2.60	0.9994
pentylbenzene	8.099	2.46	0.9989

Chemical standards were calibrated for potential use as internal, recovery, or concentration standards. Calibration curves were forced through two points: the peak area response and the origin. More points are necessary for appropriate calibration. Pristane and phytane were calibrated at 2 mg/L. The 2-fluorobiphenyl standard was calibrated at 12 mg/L. Table 4-3 includes the calibration results for pristane, phytane, and 2-fluorobiphenyl. The linear term for phytane (1.70×10^6) indicates a significant experimental error in solution preparation. The term should be similar to all other response values due to FID stability. When compared to all other linear response values, the value for phytane can be statistically rejected by Dixon's Q-test at 95% confidence (Appendix A).

Table 4-3. Summary of calibration results for chemical standards

Chemical	Retention time (min)	Linear term x 10^{-6}	Coef. of det. (r^2)
2-fluorobiphenyl	9.624	2.47	1.000
pristane	11.568	2.58	1.000
phytane	12.117	~~1.70~~	1.000

The overall average linear response term for all chemical components (excluding phytane based on Q-test rejection) was calculated to be $2.4 \times 10^6 \pm 0.2 \times 10^6$.

4.2.2 Chemical analysis of diesel

Diesel composition was characterized based on the results of the hydrocarbon calibrations (Figure B-3, Appendix B). The diesel components with the highest concentrations (excluding any unidentified chemicals) were determined to be pentadecane C15,

tetradecane C14, tridecane C13, and undecane C11. The components with the lowest concentrations were determined to be dotriacontane C32, ethylbenzene, tetracontane C40, and tetramethylbenzene. Since pristane and phytane were identified in diesel, they were deemed invalid as standards. Unidentified chemical responses in diesel were analyzed via GC-MS. Based on MS analysis, a large peak at 13.54 minutes corresponded to biodiesel (cis-9-octyldecenoic acid, methyl ester).

Diesel was calibrated for THC quantification at 5000, 2000, 500 and 300 mg/L. The THC peak was analyzed at a retention time of 12.93 minutes. Based on calibration results, the linear response term was calculated to be 2.53×10^6, with an r^2 value of 1.000. Validation of diesel calibration was performed in duplicate using a 3750 mg/L diesel solution in pentane. GC-FID responses indicated an average 4.7% difference between the experimental concentration values and the theoretical value.

4.2.3 Chemical utilization of diesel during biodegradation

Diesel hydrocarbon concentrations were analyzed throughout BOD experiments via GC analysis. Individual BOD flasks were sacrificed at designated times for liquid-solvent extraction, up-concentration, and quantization by direct GC-FID analysis.

The chromatograms from diesel calibration (refer to 4.2.2) were compared to those from time-zero extraction (3 parallels with approximately 1% precision). After samples were extracted and up-concentrated, GC-FID chromatograms were shifted slightly. The THC peak-shift indicated evaporative losses of volatile HC components. Volatile fractions were not identified in the round-bottom collection flask in the evaporation apparatus. The HCs presumably accumulated in the transfer line between evaporator and condenser. Based on the chemical analysis of the time-zero solutions and the calibration of diesel in pentane, recovery factors were determined for each calibrated chemical component. Recovery factors were calculated as follows: (theoretical diesel concentration ÷ time-zero extract diesel concentration)*(calibration concentration ÷ time-zero extract concentration)*100%. The theoretical concentration of the diesel in the time-zero extract was 9000 mg/L and the average experimental value was only 3240 mg/L.

Therefore, the recovery for diesel THC was 36% (with 64% lost in evaporation). Percent recovery values were determined for all calibrated chemical components of diesel. Values of recovery are graphically represented in Figure 4-9, plotted as a function of retention time (boiling point). The plot does not include 2-fluorobiphenyl, pristane, heptadecane C17, nonadecane C19, octacosane C28, dotriacontane C32, hexatriacontane C36, and tetracontane C40, since these fractions were not biodegraded in the test flasks.

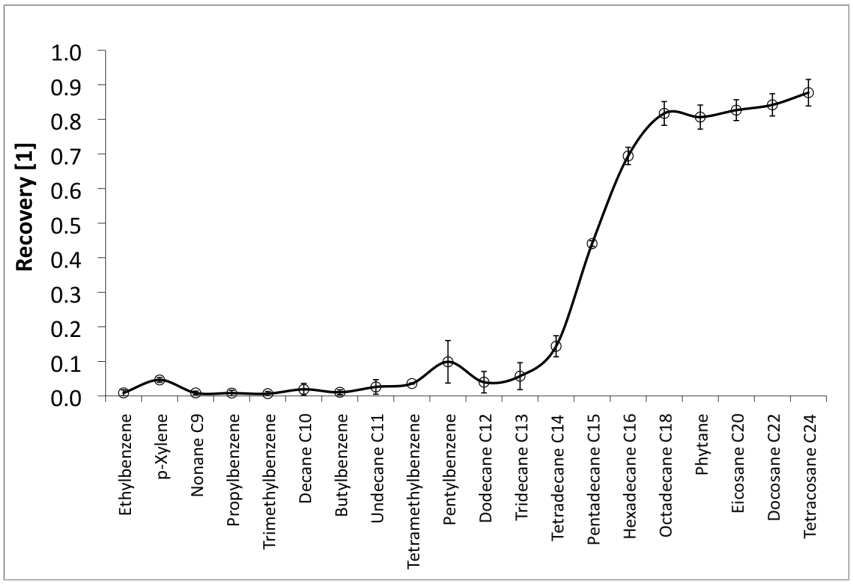

Figure 4-9. Recovery factor graph for pertinent diesel HC components based on time-zero analysis

GC-FID peak area responses from test bottle extracts were used to analyze calibrated compounds at 15, 8, 4, and 0.5°C. The GC responses from the 2-fluorobiphenyl concentration standards lacked both precision and accuracy. Therefore, the concentration standard was deemed unviable to monitor up-concentration recovery. The GC responses from all the other calibrated chemicals were used to construct degradation curves at each temperature (Figure B-4, Appendix B). Exponential trendline curves were generated, using the first several data points for best-fit trendlines. Equations of the curves were used to estimate half-life values. The half-life was defined as the time required for the original HC concentration to degrade by half.

Chemical degradation was monitored over the course of the biodegradation experiment using the exponential curves. The following components were essentially absent in the extracts: propylbenzene, dotriacontane C32, hexatriacontane C36, and tetracontane C40. The following components exhibited no trend of degradation over time: trimethylbenzene, p-xylene, ethylbenzene, nonane C9, heptadecane C17, nonadecane C19, and octacosane C28.

The following components were degraded over time at extremely low recovery (<20%): butylbenzene, tetramethylbenzene, pentylbenzene, decane C10, undecane C11, dodecane C12, and tridecane C13 (Table B-1, Appendix B). Only the half-lives from the heavy (nonvolatile) HC fractions were viable for analysis. Table 4-4 includes the half-life values for the chemical components with considerable recovery (>20%). Experimental half-life values were generally dependent on temperature and hydrocarbon chain length (Figure B-5, Appendix B).

Table 4-4. Half-life values for calibrated components with significant recovery (>20%) based on chemical degradation profiles

Chemical	Half-life (days)			
	15°C	8°C	4°C	0.5°C
tetradecane C14	0.85	5.36	2.52	4.39
pentadecane C15	0.80	5.56	2.50	3.18
hexadecane C16	1.03	6.54	3.36	3.63
octadecane C18	1.76	7.55	9.33	12.46
eicosane C20	2.21	12.51	12.67	15.31
docosane C22	2.34	15.37	12.07	15.72
tetracosane C24	2.98	13.20	18.89	27.04
pristane	4.43	6.58	11.43	22.50
phytane	5.31	11.64	20.16	27.37
diesel THC	4.47	15.74	17.46	23.58

Percent degradation curves were constructed for diesel THC at various low temperatures. Degradation percentages were calculated as follows: $1-(C/C_0)*100\%$. Figure 4-10 illustrates the degradation profiles for diesel THC over time. Based on the trendlines, half-life values were determined graphically at 50% chemical degradation. The half-lives are included in Table 4-5 for experimental validation.

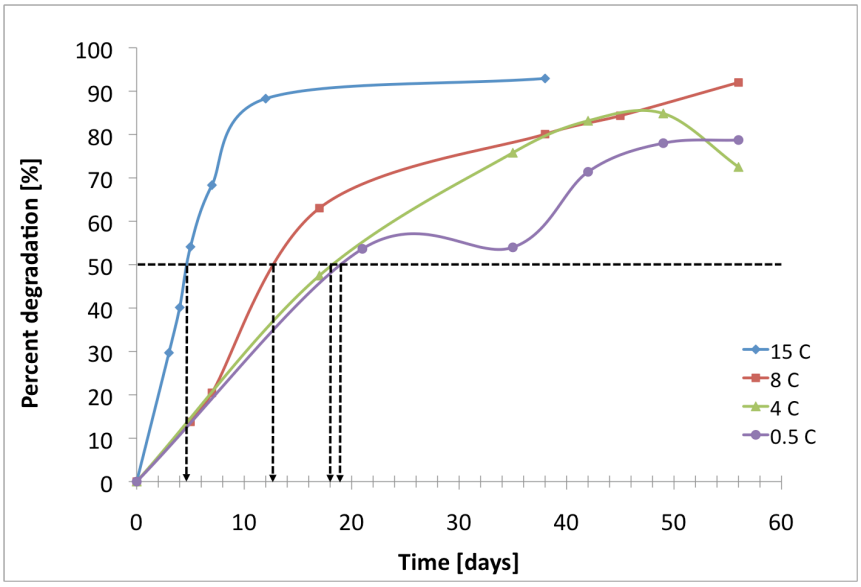

Figure 4-10. Percent degradation curve for diesel THC at 15, 8, 4, and 0.5°C

Table 4-5. Half-life values for diesel THC based on percent degradation curves

Temperature (°C)	Half-life (days)
15	4.6
8	12.7
4	18.0
0.5	19.0

4.3 TOC analysis

Positive control BOD flasks were sampled for TOC analysis. Initial TOC values were determined to be 72 mg/L based on the initial solution concentration of 199 mg/L COD or 124 mg/L sodium benzoate (COD of sodium benzoate = 1.61 g O_2/g benzoate). All measured TOC responses were multiplied by a dilution factor of 5.45 (10.9 mL total volume ÷ 2 mL sample). Appropriate blank values were then subtracted from the data. Experimental error from the triplicate TOC instrumental analysis was propagated throughout data manipulation. Due to sampling errors, the TOC samples at 0.5°C on day 14 were discarded. Parallel TOC curves were constructed at each temperature (Figures 4-11 through 4-14) and compared to BOD data from the positive control flasks. Growth parameters could not be determined graphically (i.e., from first order graphs of ln(TOC) versus time). The TOC data could only be compared qualitatively (Figure B-6, Appendix B).

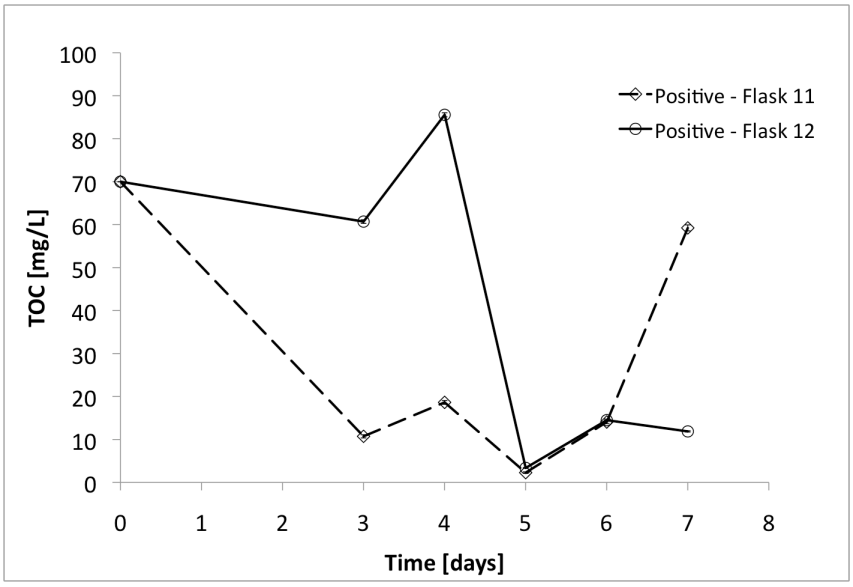

Figure 4-11. TOC curves of sodium benzoate at 15°C

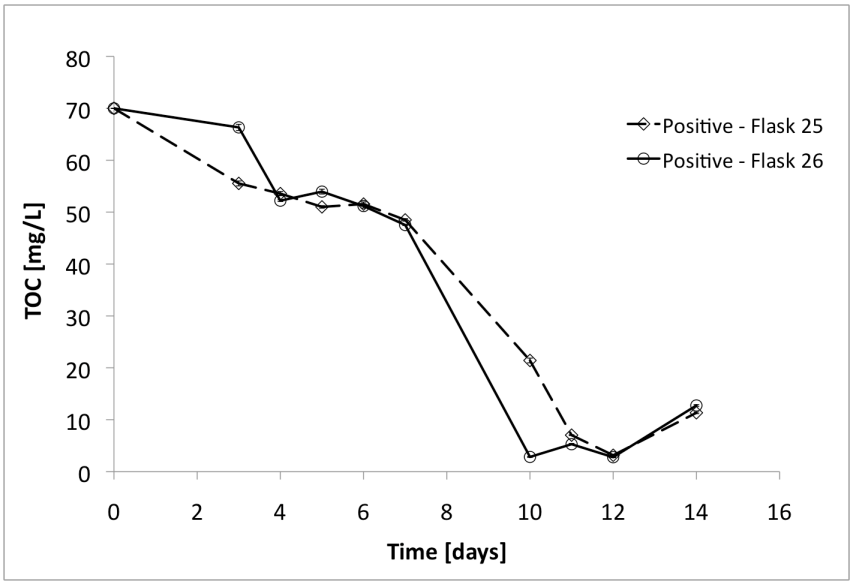

Figure 4-12. TOC curves of sodium benzoate at 8°C

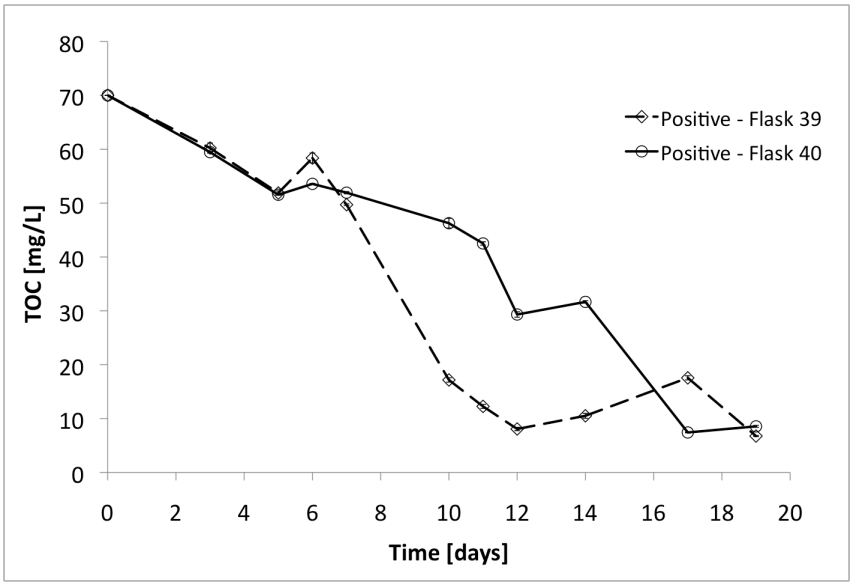

Figure 4-13. TOC curves of sodium benzoate at 4°C

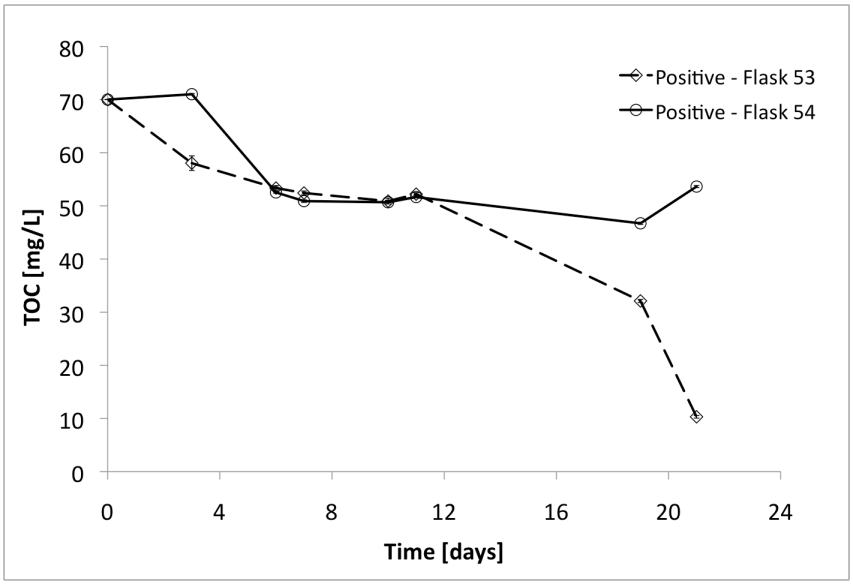

Figure 4-14. TOC curves of sodium benzoate at 0.5°C

5 DISCUSSION

The aerobic biodegradation of diesel hydrocarbons in seawater was evaluated at four temperatures: 15, 8, 4, and 0.5°C. Chemical and biological analyses were performed to enhance understanding of diesel biodegradation at low temperature. This chapter provides an overview of relevant experimental results, as well as recommendations for future analyses and implications of the present study.

5.1 Experimental errors

Errors during the biodegradation and chemical characterization of diesel were classified as either systematic or random errors. Examples of potential sources for error in solution preparation or extraction included inadequate quantitative transfer or surface adsorption. Errors in BOD analysis included cross-contamination and improper sealing of the flasks. Errors in up-concentration include the evaporation of significant quantities of petroleum hydrocarbons. Possible errors in GC analysis included contamination from excessive periods of solution storage (European Committee for Standardization, 2000). Sources for contamination in the GC-FID and MS analyses included primarily the septa (phthalates), but also potentially included the pentane solvent and column residuals. Following BOD and GC experiments, error analysis was not possible. In the future, the method should be reconfigured to include duplicate or triplicate sampling.

5.2 Analysis of diesel biodegradation (BOD/TOC)

The rates of biodegradation corresponded to temperature in the positive control systems. Positive control (sodium benzoate) flasks were evaluated in order to verify the experimental protocol for biodegradation. Biodegradation responses in BOD and TOC curves indicated parallel variations in reaction rate in each microcosm system. Sodium benzoate BOD curves illustrated longer bacterial growth lag phases at colder temperatures (Figures 4-1 to 4-4). TOC curves illustrated enhanced rates of biodegradation at higher temperature over the course of 28 days (Figures 4-11 to 4-14, Figure B-6). The final extent of biodegradation was approximately equivalent for all temperatures. Trends were generally sigmoid-shaped, due to the accumulation of inert matter in the endogenous phase. Overall, in the positive control systems, temperature positively affected the rate but not the extent of biodegradation.

The rates of degradation were also proportional to temperature in the diesel test flasks. Flasks contained immobilized diesel on Fluortex adsorbents (Brakstad and Bonaunet, 2006). Diesel BOD curves were compared qualitatively at 15, 8, 4, and 0.5°C (Figures 4-5 to 4-8, Figure B-2). Similar to the positive control system, biodegradation rates were apparently enhanced at higher temperature. However, BOD values were not significantly different at 8 and 4°C. At each temperature, variations were observed for each microcosm system. TOC analysis was not performed for the diesel samples. However, based on

extrapolation from positive control results, the extent of biodegradation was likely independent of temperature after 28 days. In order to assess the final extent of mineralization of diesel petroleum hydrocarbons after 64 days, TOC analyses ought to be performed for diesel test flasks throughout the course of biodegradation. Diesel biodegradation results are consistent with the hydrocarbon trends from several recently published studies (Brakstad and Bonaunet, 2006; Michaud et al., 2004; Mohn and Stewart, 2000).

5.3 Analysis of hydrocarbon utilization (GC)

Prior to chemical analysis of experimental samples, petroleum hydrocarbons and diesel THC responses from GC-FID were calibrated and characterized. Calibrations were generally successful, with consistently linear response terms. The erroneous linear response for phytane indicated significant systematic error in solution preparation. A validation was performed only for diesel THC to demonstrate the accuracy of the calibration method. GC-FID and MS analyses were used for diesel characterization. The components with the highest concentrations in diesel were identified as alkanes (C11 to C15). This is reasonable, based on the assumption that petroleum diesel consists mainly of saturated hydrocarbons (Margesin and Schinner, 2001; Widdel and Rabus, 2001). The diesel components with the lowest concentrations were identified as substituted aromatics (ethylbenzene and tetramethylbenzene) and high molecular weight alkanes (C32 and C40). More extensive MS analysis is necessary for thorough characterization of diesel.

The chemical standards of pristane, phytane, and 2-fluorobiphenyl were determined to be unviable in analysis. Pristane and phytane were identified in diesel and, contradictory to the findings of Whyte et al., were observed to biodegrade over time (1998). The 2-fluorobiphenyl standard was deemed unviable to measure up-concentration recovery, due to imprecise, inaccurate GC-FID responses from co-elution, adsorption to hydrophobic surfaces, and evaporation. In future experiments, more appropriate (e.g., unbiodegradable, non-fluorinated) standards should be developed for use as internal, recovery, and concentration standards.

The chemical utilization of petroleum hydrocarbons during biodegradation was determined to be temperature dependent. Reactions were assumed to follow first order Monod kinetics,

due to the low solubility of the HC diesel components (Appendix A). Recovery factors were calculated for each component HC, since 64% of diesel components were lost in evaporation. Generally, the recovery factors were correlated to individual boiling points (or retention times) of the HC components (Figure 4-9). During the up-concentration, volatile HCs presumably accumulated in the transfer line between evaporator and condenser. Based on the evaporative losses of essential petroleum hydrocarbons, the evaporation procedure was classified as a methodological failure. In future analyses, the evaporation should take place at ambient room temperature (Delille et al., 2009).

Conversely, GC-FID responses were stable with approximately 1% precision for diesel THC extracts at time zero. Degradation curves (Figure B-4) were constructed for each HC component, based on GC peak area responses. Half-life values were calculated at each temperature according to presumably exponential degradation. Only the half-lives from the heavy (nonvolatile) HC fractions were viable for analysis (Table 4-4). Percent biodegradation trends were constructed for petroleum THC to calculate new half-life values and analyze mineralization at each temperature (Michaud et al., 2004). Half-lives determined by the two methods were comparable and were used to evaluate the rates and extent of chemical utilization. Experimental half-life values were generally dependent on temperature and hydrocarbon chain length. Specifically, the half-lives were directly proportional to HC length and inversely proportional to temperature (Figure B-5, Appendix B).

Therefore, the rates of HC utilization depended on both temperature and chemical structure. This is consistent with recent studies showing that short chain alkanes are metabolized faster than long chain hydrocarbons at low temperature (Deppe et al., 2005; Jobson et al., 1972; Lin et al., 2009; Lindstrom and Braddock, 2002; Whyte et al., 1998). However, the final extent of utilization was apparently unaffected by temperature after significant incubation periods (refer to 5.2).

5.4 Further investigations

Based on incomplete results from the biodegradation of diesel in seawater, further analyses and experiments are recommended. Kinetic parameters should be determined by graphical comparison of individual BOD curves or by mathematical modeling. Simulated

mathematical models (e.g., AQUASIM) could be used for data simulation, parameter estimation, and uncertainty analysis based on diesel biodegradation (Reichert, 1998). Models should account for compartmental partitioning of the Fluortex filter. Additionally, bacterial enumeration should be performed using DAPI epifluorescence microscopy. Finally, bioremediation techniques should be researched and evaluated during diesel biodegradation analysis in seawater at low temperatures.

5.5 Implications

Laboratory experiments ought to be developed (refer to 5.4) in order to ultimately extrapolate results to natural systems. However, a synergy of factors (e.g., sunlight, water current, predation, etc.) complicates biodegradation in nature (refer to 2.2-2.3). Despite these limitations of extrapolation to real world systems, an obvious recommendation involves urgent decreases in petroleum inputs into the ocean. Since the rate of diesel HC biodegradation is directly proportional to temperature, petroleum HCs are probably more recalcitrant in low temperature marine ecosystems (depending on the exact conditions). This trend may help forecast marine biodegradation rates during ocean temperature changes associated with global warming. Additionally, if degradation is slowed tremendously at cold temperature, offshore petroleum development in high latitude regions may come with substantial risk. Further analysis is required for offshore environmental risk assessments.

6 CONCLUSION

The aerobic biodegradation of petroleum diesel hydrocarbons was evaluated in seawater at low temperatures. Specifically, biological oxygen demand and chemical utilization were monitored over a period of 64 days in sealed, microcosm systems. Substrate analyses of saturated, aromatic, and total hydrocarbons were examined via extraction, evaporation, and gas chromatography analysis. The quantitative biological and chemical analyses were performed to ultimately enhance understanding of diesel biodegradation and utilization in cold marine environments.

The primary conclusions are as follows:

1) According to qualitative BOD and TOC data, sodium benzoate (positive control) biodegradation was determined to be temperature dependent. The rates of biodegradation were enhanced at higher temperature; however, the extent of degradation was essentially temperature independent. Based on qualitative BOD analysis, diesel biodegradation was also temperature dependent. However, BOD values were not significantly different at 8 and 4°C.
2) Chemical standards of pristane, phytane, and 2-fluorobiphenyl were deemed invalid as internal, reference, and concentration standards, respectively.
3) The chemical profile of diesel included high concentrations of various saturated hydrocarbons and low concentrations of substituted aromatics and high molecular weight alkanes.
4) The up-concentration procedure was a methodological failure, causing evaporative losses of volatile petroleum hydrocarbons. The calculated recovery for diesel THC was 36% (with 64% losses in evaporation).
5) According to calculated half-life values for diesel chemical constituents, the rates of HC utilization depended on both temperature and chemical structure. Typically, the rates of utilization are directly proportional to temperature and inversely proportional to hydrocarbon chain length. The extent of mineralization was temperature independent after significant incubation periods.
6) Future research is necessary to better understand the natural processes of microbial degradation of diesel in seawater at low temperature and to effectively enhance these rates through bioremediation.

7 REFERENCES

AISLABIE, J., SAUL, D. J. & FOGHT, J. M. (2006) Bioremediation of hydrocarbon-contaminated polar soils. *Extremophiles,* 10**,** 171-179.

ALDRETT, S., BONNER, J. S., MILLS, M. A., AUTENRIETH, R. L. & STEPHENS, F. L. (1997) Microbial degradation of crude oil in marine environments tested in a flask experiment. *Water Research,* 31**,** 2840-2848.

ATLAS, R. M. (1981) Microbial Degradation of Petroleum Hydrocarbons: an Environmental Perspective. *Microbiological Reviews,* 45**,** 180-209.

ATLAS, R. M. (1995) Petroleum Biodegradation and Oil Spill Bioremediation. *Marine Pollution Bulletin,* 31**,** 178-182.

BRAKSTAD, O. G. & BONAUNET, K. (2006) Biodegradation of petroleum hydrocarbons in seawater at low temperatures (0-5 °C) and bacterial communities associated with degradation. *Biodegradation,* 17**,** 71-82.

BRIERLEY, A. & KINGSFORD, M. (2009) Impacts of Climate Change on Marine Organisms and Ecosystems. *Current Biology,* 19**,** R602-R614.

DEAN, J. A. (1995) *Analytical Chemistry Handbook*, McGraw-Hill Inc., New York, 4.1-4.63.

DELILLE, D., PELLETIER, E., RODRIGUEZ-BLANCO, A. & GHIGLIONE, J. F. (2009) Effects of nutrient and temperature on degradation of petroleum hydrocarbons in sub-Antarctic coastal seawater. *Polar Biology,* 32**,** 1521-1528.

DEPPE, U., RICHNOW, H. H., MICHAELIS, W. & ANTRANIKIAN, G. (2005) Degradation of crude oil by an arctic microbial consortium. *Extremophiles,* 9**,** 461-470.

EUROPEAN COMMITTEE FOR STANDARDIZATION (2000) Water quality, Determination of hydrocarbon oil index, Part 2: Method using solvent extraction and gas chromatography, ISO 9377-2.

GEERDINK, M. J., VAN LOOSDRECHT, M. & LUYBEN, K. (1996) Biodegradability of diesel oil. *Biodegradation,* 7, 73-81.

JOBSON, A., COOK, F. D. & WESTLAKE, D. W. S. (1972) Microbial Utilization of Crude Oil. *Applied Microbiology,* 23, 1082-1089.

KLOOS, K., SCHLOTER, M. & MEYER, O. (2006) Microbial activity in an acid resin deposit: Biodegradation potential and ecotoxicology in an extremely acidic hydrocarbon contamination. *Environmental Pollution,* 144**,** 136-144.

LEAHY, J. G. & COLWELL, R. R. (1990) Microbial Degradation of Hydrocarbons in the Environment. *Microbiological Reviews,* 54**,** 305-315.

LEE, R. F. & PAGE, D. S. (1997) Petroleum Hydrocarbons and Their Effects in Subtidal Regions after Major Oil Spills. *Marine Pollution Bulletin,* 34**,** 928-940.

LIN, X. Z., YANG, B. J., SHEN, J. H. & DU, N. (2009) Biodegradation of Crude Oil by an Arctic Psychrotrophic Bacterium Pseudoalteromomas sp. P29. *Current Microbiology,* 59**,** 341-345.

LINDSTROM, J. E. & BRADDOCK, J. F. (2002) Biodegradation of petroleum hydrocarbons at low temperature in the presence of the dispersant Corexit 9500. *Marine Pollution Bulletin,* 44**,** 739-747.

MARGESIN, R. & SCHINNER, F. (2001) Biodegradation and bioremediation of hydrocarbons in extreme environments. *Applied Microbiology and Biotechnology,* 56**,** 650-663.

MICHAUD, L., LO GIUDICE, A., SAITTA, M., DE DOMENICO, M. & BRUNI, V. (2004) The biodegradation efficiency on diesel oil by two psychrotrophic Antarctic marine bacteria during a two-month-long experiment. *Marine Pollution Bulletin,* 49**,** 405-409.

MITRA, S. (2003) *Sample Preparation Techniques in Analytical Chemistry,* Hoboken, N.J., J. Wiley.

MOHN, W. W. & STEWART, G. R. (2000) Limiting factors for hydrocarbon biodegradation at low temperature in Arctic soils. *Soil Biology & Biochemistry,* 32**,** 1161-1172.

MultiPurposeSampler Operation Manual (2000) Gerstel GmbH & Co., Germany.

NATIONAL RESEARCH COUNCIL (1985) *Oil in the sea: inputs, fates, and effects,* Washington, D.C., National Academy Press.

NICHOLS, D., BOWMAN, J., SANDERSON, K., NICHOLS, C. M., LEWIS, T., MCMEEKIN, T. & NICHOLS, P. D. (1999) Developments with Antarctic microorganisms: culture collections, bioactivity screening, taxonomy, PUFA production and cold-adapted enzymes. *Current Opinion in Biotechnology,* 10**,** 240-246.

OxiTop System Control Operating Manual (2006) WTW Weilheim, Germany.

POWELL, S. M., HARVEY, P. M., STARK, J. S., SNAPE, I. & RIDDLE, M. J. (2007) Biodegradation of petroleum products in experimental plots in Antarctic marine sediments is location dependent. *Marine Pollution Bulletin,* 54, 434-440.

REICHERT, P. (1998) AQUASIM 2.0 User Manual: Computer program for the identification and simulation of aquatic systems. *Swiss Federal Institute for Environmental Science and Technology.*

RORABACHER, D. B. (1991) Statistical Treatment for Rejection of Deviant Values: Critical Values of Dixon's "Q" Parameter and Related Subrange Ratios at the 95% Confidence Level. *Analytical Chemistry,* 63, 139-146.

ROSENBERG, E., LEGMANN, R., KUSHMARO, A., TAUBE, R., ADLER, E. & RON, E. Z. (1992) Petroleum bioremediation - a multiphase problem. *Biodegradation,* 3**,** 337-350.

SHERR, B., SHERR, E. & DEL GIORGIO, P. (2001) Enumeration of Total and Highly Active Bacteria. *Methods in Microbiology,* 30, 129-159.

VIEIRA, P. A., VIEIRA, R. B., DE FRANCA, F. P. & CARDOSO, V. L. (2007) Biodegradation of effluent contaminated with diesel fuel and gasoline. *Journal of Hazardous Materials*, 140, 52-59.

WALKER, C. H., HOPKIN, S. P., SIBLY, R. M. & PEAKALL, D. B. (2006) *Principles of Ecotoxicology,* Boca Raton, Taylor & Francis.

WHYTE, L. G., HAWARI, J., ZHOU, E., BOURBONNIERE, L., INNISS, W. E. & GREER, C. W. (1998) Biodegradation of Variable-Chain-Length Alkanes at Low Temperatures by a Psychrotrophic Rhodococcus sp. *Applied and Environmental Microbiology,* 64**,** 2578-2584.

WIDDEL, F. & RABUS, R. (2001) Anaerobic biodegradation of saturated and aromatic hydrocarbons. *Current Opinion in Biotechnology,* 12**,** 259-276.

YANG, L., LAI, C. T. & SHIEH, W. K. (2000) Biodegradation of dispersed diesel fuel under high salinity conditions. *Water Research,* 34, 3303-3314.

APPENDIX A: THEORETICAL INFORMATION

Supplemental equations and theoretical descriptions are included in this chapter. All theories are referenced in the main text.

Monod kinetics:

$$u = u_{\max} \frac{S}{K_S + S}$$

where $S << K_s$

Arrhenius equation:

$$k = Ae^{E_a / RT}$$

k	Rate constant
A	Pre-exponential factor
E_a	Activation energy (J/mol)
R	Gas constant (8.314 J/mol·K)
T	Temperature (K)

Relationship between BOD and pressure (*OxiTop System Control Operating Manual*, 2006):

$$BOD = \frac{MW(O_2)}{R \cdot T_m} \cdot \left(\frac{V_t - V_l}{V_l} + \alpha \frac{T_m}{T_0} \right) \cdot \Delta p(O_2)$$

$MW(O_2)$	Molecular weight (32 000 mg/mol)
R	Gas constant (83.14 L·mbar/mol·K)
T_0	Reference temperature (273.15 K)
T_m	Measuring temperature (K)
V_t	Bottle volume (mL)
V_l	Sample volume (mL)
α	Bunsen absorption coefficient (0.0310)
$\Delta p(O_2)$	Difference in oxygen partial pressure (mbar)

Dixon's Q-test (Rorabacher, 1991):

$$Q_{\text{exp}} = \frac{x_N - x_{N-1}}{x_N - x_1}$$

Q_{exp}	Calculated Q-value
x_N	Suspected outlier
x_{N-1}	Value nearest to the outlier
$(x_N - x_1)$	Range of values in the data set

Critical Q-values (Q_{crit}) are provided in statistical literature at varying confidence levels. Table A-1 includes literature Q_{crit} values at the 95% confidence level. If Q_{exp} is greater than Q_{crit}, the suspected outlier can be rejected.

Table A-1. Q_{crit} values at 95% confidence level (Rorabacher, 1991)

Number of observations, N	Q_{crit} value
3	0.970
4	0.829
5	0.710
6	0.625
7	0.568
8	0.526
9	0.493
10	0.466
15	0.384
20	0.342
25	0.317
30	0.298

APPENDIX B: EXPERIMENTAL INFORMATION

Supplemental information from the biodegradation experiment and analysis are included in this chapter. Figures and tables are referenced in the main text.

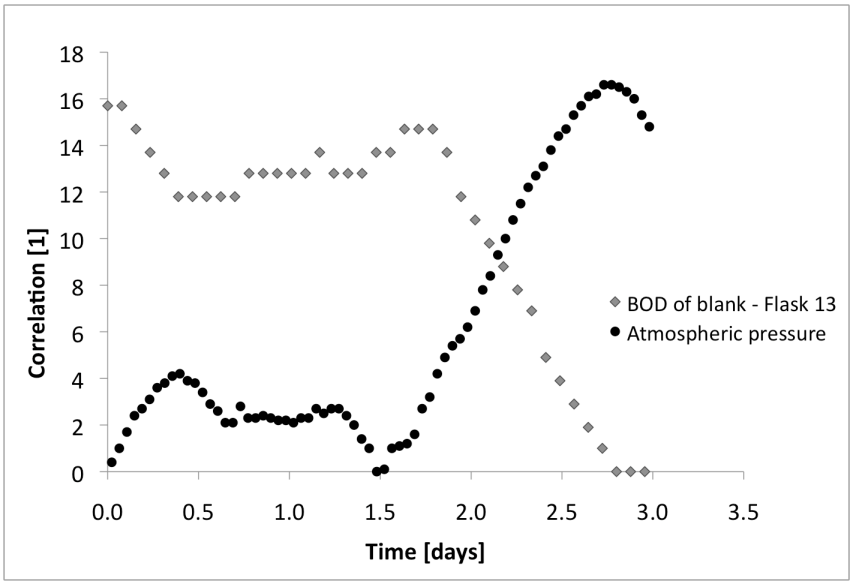

Figure B-1. Normalized negative correlation of atmospheric pressure and BOD from an open blank flask at 15°C

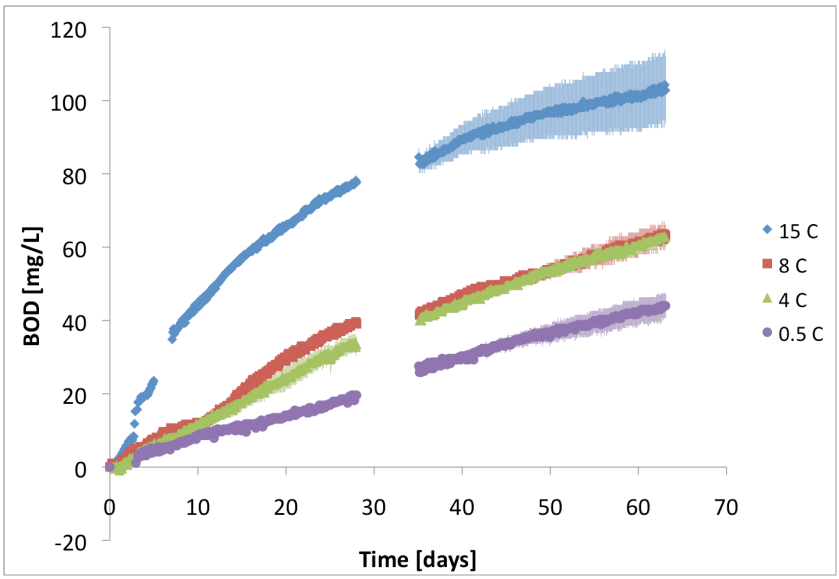

Figure B-2. Comparative, temperature-dependent diesel BOD curve, for simple visualization only

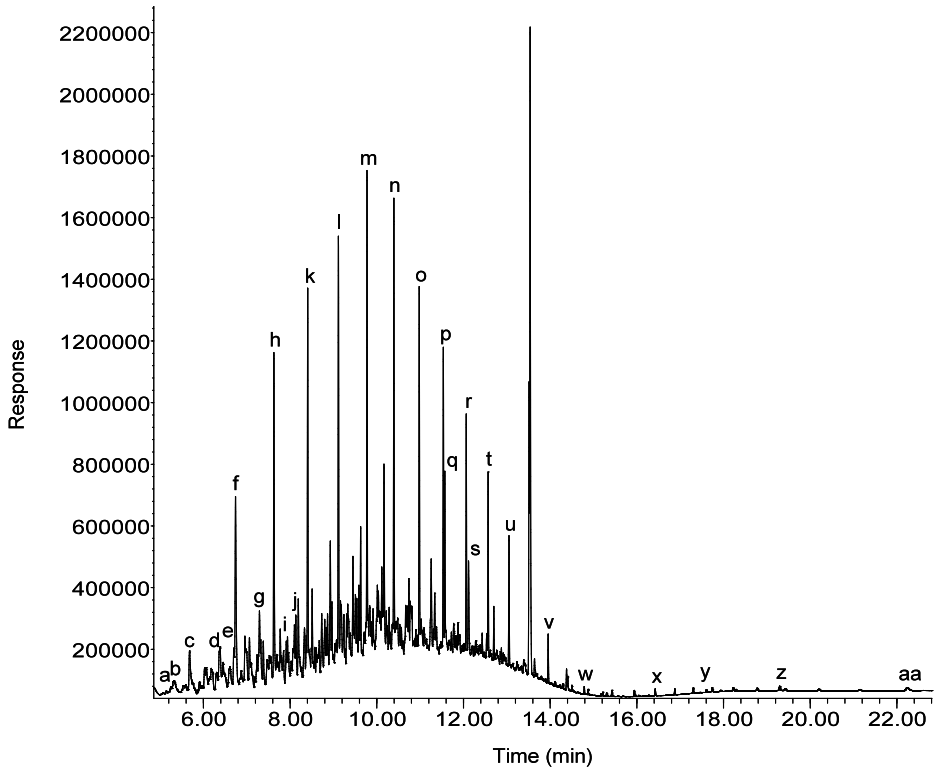

Figure B-3. Sample GC-FID chromatogram of diesel in pentane (300 mg/L)
Legend: ethylbenzene (a), p-xylene (b), nonane (c), propylbenzene (d), trimethylbenzene (e), decane (f), butylbenzene (g), undecane (h), tetramethylbenzene (i), pentylbenzene (j), dodecane (k), tridecane (l), tetradecane (m), pentadecane (n), hexadecane (o), heptadecane (p), pristane (q), octadecane (r), phytane (s), nonadecane (t), eicosane (u), docosane (v), tetracosane (w), octacosane (x), dotriacontane (y), hexatriacontane (z), tetracontane (aa)

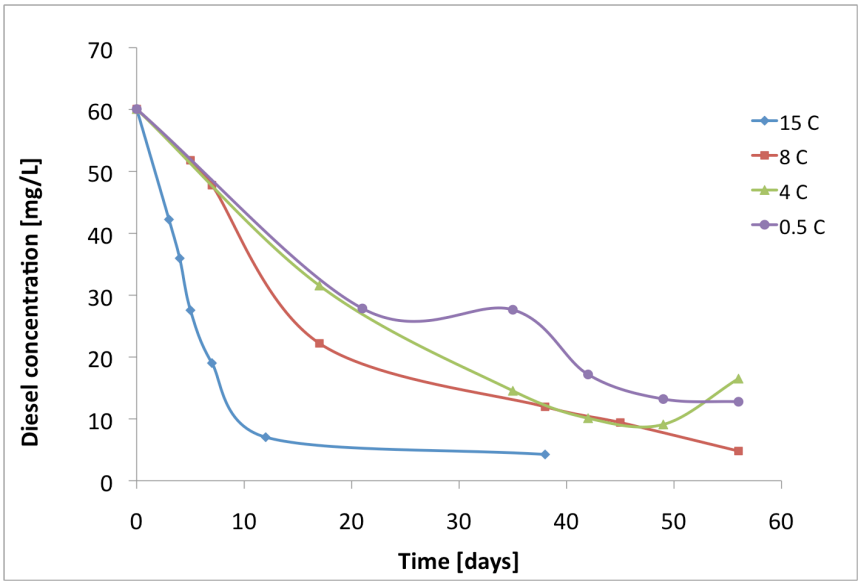

Figure B-4. Degradation curve for diesel THC concentrations at 15, 8, 4, and 0.5°C

Table B-1. Half-life values for calibrated chemical components with low recovery (<20%)

Chemical	Half-life (days)			
	15°C	8°C	4°C	0.5°C
butylbenzene	1.93	3.28	N/A	N/A
tetramethylbenzene	1.17	2.15	5.59	N/A
pentylbenzene	1.01	2.13	N/A	7.37
decane C10	0.71	1.15	N/A	N/A
undecane C11	0.97	1.86	3.30	7.44
dodecane C12	0.95	2.03	10.27	7.72
tridecane C13	0.96	2.64	2.69	6.93

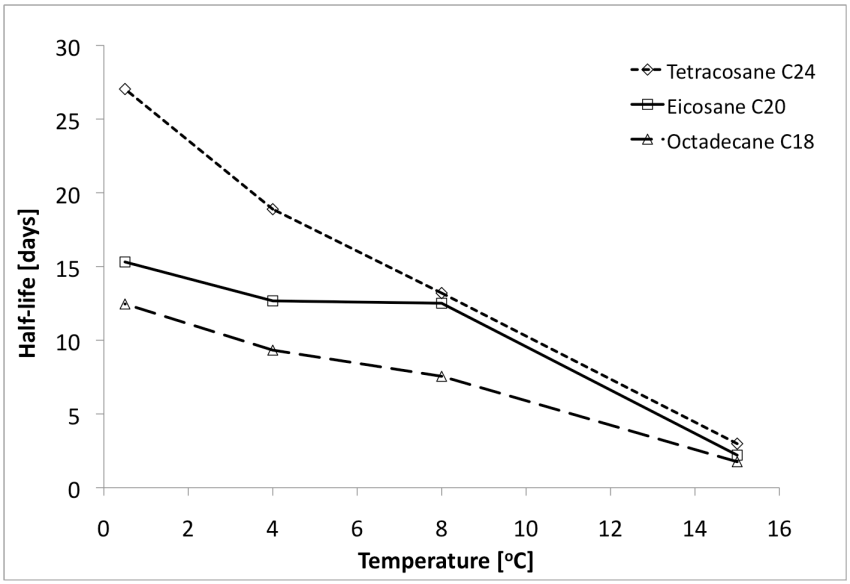

Figure B-5. Half-life dependence on temperature and hydrocarbon chain length, for visualization only

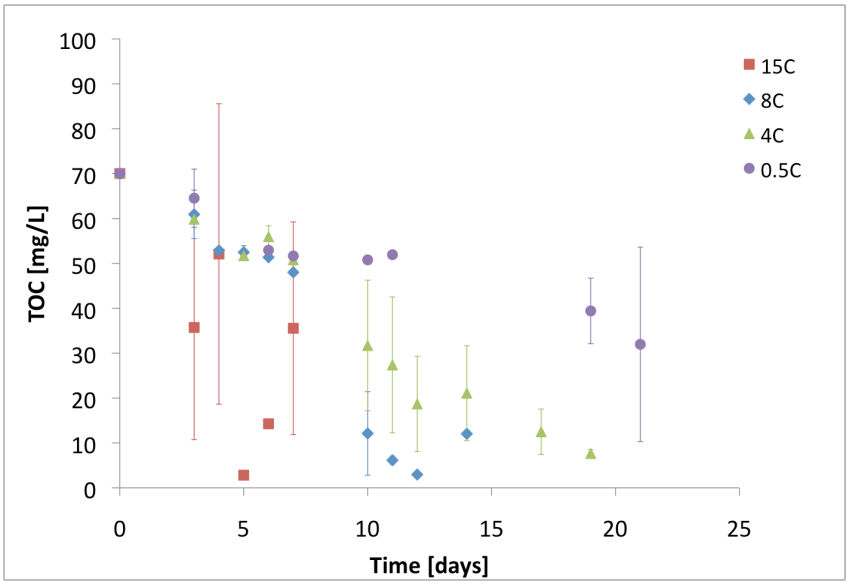

Figure B-6. Comparative, averaged sodium benzoate TOC data, for simple visualization only